Hydroclimate variability in Scandinavia over the last millennium - insights from a climate model-proxy data comparison

Kristina Seftigen[1,2,*], Hugues Goosse[2], Francois Klein[2], Deliang Chen[1]

[1]Regional Climate Group, Department of Earth Sciences, University of Gothenburg, Gothenburg, Sweden.

[2]Georges Lemaître Centre for Earth and Climate Research (TECLIM), Earth and Life Institute, Université catholique de Louvain (UCL), Belgium.

[*]Corresponding author:

E-mail address: kristina.seftigen@gvc.gu.se

Abstract

The integration of climate proxy information with General Circulation Model (GCM) results offers considerable potential for deriving greater understanding of the mechanisms underlying climate variability, as well as unique opportunities for out-of-sample evaluations of model performance. In this study, we combine insights from a new tree-ring hydroclimate reconstruction from Scandinavia with projections from a suite of forced transient simulations of the last millennium and historical intervals from the CMIP5 and PMIP3 archives. Model simulations and proxy reconstruction data are found to broadly agree on the modes of atmospheric variability that produces droughts/pluvials in the region. Despite these dynamical similarities, large differences between simulated and reconstructed hydroclimate time series remain. We find that the GCMs simulated multidecadal/longer hydroclimate variability is systematically smaller than the proxy based estimates, whereas the dominance of GCM simulated high-frequency components of variability is not reflected in the proxy record. Furthermore, the paleoclimate evidence indicates in-phase coherencies between regional hydroclimate and temperature on decadal time-scales, i.e. sustained wet periods have often been concurrent with warm periods and vice versa. The CMIP5/PMIP3 archive suggests, on the other hand, out-of-phase coherencies between the two variables in the last millennium. The lack of adequate understanding of mechanisms linking temperature and moisture supply on longer time scales has serious implications for attribution and prediction of regional hydroclimate changes. Our findings stresses the need for further paleoclimate-data model intercomparison efforts to expand our understanding of the dynamics of hydroclimate variability and change, to enhance our ability to evaluate climate models, and to provide a more comprehensive view of future drought and pluvial risks.

1. Introduction

Among the current key priorities in climate research is a more comprehensive understanding of changes in regional- to continental-scale hydroclimate in response to rising levels of atmospheric greenhouse gases on time scales ranging from decades to centuries (Wu et al., 2013; Hegerl et al., 2015). Delineating the role of internal variability and natural forcing, and its contribution to the anthropogenically forced twentieth century climate (Zhang et al., 2007; Sarojini et al., 2016), is immensely important for attributing past and predicting future trajectories in the hydrological cycle, and for strategic approaches to adaptation and planning. Sparse observational evidences limits possibilities of providing tight constraints on the long-term behavior of the climate system. The longest instrumental records (~150-200 years) are too short to fully sample modes of variability that are either rare or occur on multidecadal-to-centennial timescales. This motivates the development of paleoclimatic proxy reconstructions, which extends the observational baseline into the longer spectrum of climate variability and provides a framework to consider both internal and forced climate changes.

Considerable advancements have recently been made in developing tree-ring estimates of late Holocene hydroclimate variability across Scandinavia (Seftigen et al., 2014; Cook et al., 2015). Being located in the high-latitude boreal zone, Scandinavia is well suited for dendroclimatological studies and has a long tradition of climate and environmental research using tree-ring data (Linderholm et al., 2010). The use of tree-ring proxy evidence to study natural hydroclimate variability has however long been secondary when compared to the scientific attention focused on providing local/regional reconstructions (Gunnarson et al., 2011; Esper et al., 2012; McCarroll et al., 2013; Linderholm et al., 2014) and methodologies (Björklund et al., 2012; 2014) to study temperature variability over the last several millennia. Much of the tree-ring research at moisture-limited sites have until recently been limited to a handful of exploratory papers (Helama and Lindholm, 2003; Linderholm et al., 2004; Jönsson and Nilsson, 2009; Drobyshev et al., 2011; Seftigen et al., 2013) that generally develop one or few chronologies to provide local precipitation/drought histories. These studies, together with a steadily growing collection of high-latitude moisture sensitive tree-ring records (e.g., Seftigen et al., 2015), now serves as a basis for new possibilities to expand the detail and accuracy with which the history of Northern European moisture conditions can be described.

A recent milestone in the field include the development of the “Old World Drought Atlas” ("OWDA", Cook et al., 2015), a set of tree-ring reconstructed year-to-year maps that provide temporal *and* spatial details of droughts and wetness in the last millennium across Europe,

including Scandinavia. The OWDA has been used to elucidate hydroclimatic blueprints of the Medieval Climate Anomaly (MCA, ~1000-1200 CE). Aligning with prior findings (Helama et al., 2009), the atlas reveals the occurrence of so-called megadroughts in large portions of continental north-central Europe and southern Scandinavia during the MCA period. Interestingly, MCA and other "Old World" droughts seem to coincide with the timing of some severe and persistent droughts documented in the climate history of North America. While this suggests the presence of some common driving mechanisms across the North Atlantic, being possibly related to variations in the Atlantic Ocean SST or/and the North Atlantic Oscillation (Feng et al., 2011; Oglesby et al., 2012), the cause of these megadroughts remains to be an open question.

While the proxy reconstructions undoubtedly play a pivotal role in unraveling statistical qualities of past climate, they are, alone, not able to provide a comprehensive view of the underlying physics governing the climate system. The forced-transient simulations over the last millennium from fully coupled general circulation models (GCMs) (Taylor et al., 2012) therefore offer an important complementary approach to the empirical analyses of proxy estimates. Paleoclimate reconstructions provide an observational basis that spans beyond current climate conditions that were used in developing and tuning such numerical models, thus allowing for out-of-sample evaluations of the models' predictive power. The models, on the other hand, can be used to explore the dynamics that have driven climate variability in the past.

This paper builds on previous tree-ring analyses (Seftigen et al., 2014; 2015) and aims at employing a paleoclimate-data model comparison framework to further explore the drivers and dynamics of drought/pluvials across Northern Europe. We analyze an ensemble of six state-of-the-art GCMs from the Past Model Intercomparison Phase 3 (Schmidt et al., 2011 - PMIP3) and the Coupled Model Intercomparison Phase 5 (Taylor et al., 2012 - CMIP5) and compare them to a new regional tree-ring-based proxy reconstruction of drought and wetness, spanning the last millennium of the Common Era (CE). A combined data approach is used to (1) evaluate to what extent the GCMs are capable in reproducing the key features of the paleoclimate record, and (2) to estimate the role of external forcing versus internal variability in driving the hydroclimatic changes regionally. The relative contribution of changes in rainfall and surface temperature at inter-annual and decadal/longer time-scales to regional hydroclimate patterns is also briefly explored, and the ability of the CMIP5/PMIP3 models to simulate the mechanisms by which the regional hydroclimate is constrained by these two variables are evaluated. The collective proxy-model data assessment will help to increase our

understanding of decadal/longer climate dynamics in regions and to evaluate the ability of the state-of-the-art GCMs to simulate realistic future hydroclimatology regionally and across a variety of different timescales.

The paper is structured as follows. Sect. 2 reviews the methods and describes the paleoclimate and CMIP5/PMIP3 datasets. Subsequent analyses concentrates on comparing the GCM simulations with the proxy based hydroclimate reconstructions (sect. 3), and delineating the role of external (sect. 4) and internal (sect. 5) sources of variability over the last millennium. The principal results and the implication of this study are discussed in sect. 6.

2. Data and methods

2.1 CMIP5/PMIP3 simulations

Simulations with six models (CESM1, CCSM4, IPSL-CM5A-LR, MIROC-ESM, MPI-ESM-P, BCC-CSM1-1) contributing to the Coupled and Paleo Model Intercomparison Projects Phases (CMIP3/PMIP3) (Schmidt et al., 2011; Taylor et al., 2012) have been used (Table I). The analyses were restricted to models that have available complete monthly precipitation and temperature variables spanning the last millennium (850-1849 CE) through historical (1850-2005 CE) time intervals. The six millennium simulations were forced with reconstructed solar, volcanic, greenhouse gas (GHG) and aerosol forcing, and partly land use changes, whereas the historical simulations included natural and anthropogenic forcing (Schmidt et al., 2011; Taylor et al., 2012). Except for CESM1, the analyses were limited to the first r1i1p1 ensemble member. Supplementary information (sect. S1, Fig. S1) provide an evaluation of six selected model rainfall and temperature simulations against instrumental reference data focusing on the northern European sector.

2.2. Proxy data

The use of annually resolved tree-ring series in the study of past hydroclimate variations has traditionally been confined to lower-latitude arid and semi-arid region, with only a few exceptions for the northern European sector. This is because the influence of moisture on tree-growth generally decreases and is successively replaced by sensitivity to warm-season temperature towards northern, cooler and wetter environment. Nevertheless, a growing body of research (e.g., Helama and Lindholm, 2003; Wilson et al., 2012; Seftigen et al., 2013) has established the potential to develop moisture-sensitive tree-ring chronologies in high-latitude environments if a careful selection of species and sites is made. Building upon these findings,

we here analyse an existing network (Seftigen et al., 2014; 2015) of 25 *Pinus sylvestris* L. tree-ring width chronologies from across a number of dry sites in southern Scandinavia (Fig. 1). The collected trees have typically been growing on well-drained soils or steep south-facing slopes with warm and sunny exposure. Thus low soil moisture availability during the growing season has been shown to be the most common growth-limiting factor in the tree-ring network (Fig. S3 and S6).

The start dates of the chronologies varied across the collection, ranging from 532 to 1790 CE (Table II). All chronologies extended at least to year 1995. In order to reduce the risk of natural/anthropogenic disturbance signal from inflicting non-climate noise upon the reconstruction, the tree-ring data has been standardized in previous research (Seftigen et al., 2014) by using a flexible "data-adaptive" method of standardization (Cook et al., 1995). This has limited the degree to which longer-timescale climate information can be extracted. Therefore, rather than using the already available hydroclimate reconstruction provided in Seftigen et al. (2014), we have here re-processed the TRW collection with the newest signal-free (SF) method of standardization (Melvin and Briffa, 2008), which has the capacity of preserving long-term variability due to climate changes. The standardization was performed with the ARSTAN software (Cook and Krusic, 2005). Chronologies combining living and historical/subfossil material were standardized with a regional curve standardization (RCS) approach (Briffa et al., 1992), applying a single RCS curve without any pith-offset adjustments to detrend all series. To avoid spurious growth trends in the resulting RCS chronologies stemming from a modern sample bias (Briffa and Melvin, 2011), tree-ring datasets based only on living trees were standardized using the SF method in combination with an age-dependent smoothing spline applied individually to each series. Prior to the standardization, the modern chronology data were high-pass filtered and subsequently grouped by means of a S-mode principal component analysis over the common interval (1792 – 1996 CE). The resulting eigenvector loadings are provided in supplemental material (Fig. S2) and describe the major modes of high-frequency variability within the multiple modern chronologies composing the dataset. The subdivision of the chronologies essentially identified an east-west pattern, broadly corresponding to sub-regional differences in topography and climate across the study domain. This suggested that the sub-regional tree-growth coherence at high frequencies was driven by climate. Hence, it would be rational to expect a common, climatically induced, growth variability also at the medium-frequency time scales, while any disparities in the sub-regional tree-growth signal are likely mostly non-climatic in origin (i.e. local site management practices, stand dynamics or other 'random' site-specific disturbances).

Therefore, in order to remove or minimize undesirable non-climatic noise upon our dataset, modern tree-ring series were first merged group-wise as identified by the first four principal components and subsequently detrended as four separate 'batches' using the SF method. The standard version of the resulting tree-growth indices were subsequently separated and averaged for each site to produce individual site chronologies. This procedure enabled us to retain any shared, sub-regional, growth-forcing signal while removing site-specific medium- to high-frequency noise.

Final data were adjusted to reduce the variance bias stemming from varying sample size trough time (Frank et al., 2006). The resulting chronologies were truncated where the Expressed Population Signal (EPS) (Wigley et al., 1984) dropped below the 0.85 threshold, or, in case of the longer chronologies, at year 1000 CE. The median segment length (MSL) of all the chronologies (Table II) ranged between 74 and 357 years, and the median MSL across all sites was 197 years. Although a precise quantification of returned frequency variance in the final SF detrended tree-ring chronologies was not straightforward, the median MSL suggested that it should be possible to use the network to reconstruct climate variability at time scales up to ~200 years.

2.3. Regional hydroclimatology

The CMIP5/PMIP3 inter-model spread in spatial resolution and sophistication of soil moisture schemes makes meaningful inter-model comparison difficult. To bypass some of these challenges, the Standardized Precipitation Evapotranspiration Index (SPEI) (Vicente-Serrano et al., 2013) was used to characterize the regional hydroclimatology across the study domain. The SPEI, a commonly used metric of soil moisture balance, has successfully been used as a target variable in several prior tree-ring reconstructions (e.g., Seftigen et al., 2014; 2015). The index is not a state variable but rather an offline metric of the surface moisture balance that can be consistently derived across models and therefore provide standard measure of hydroclimatic variability across GCMs. The computation of the index is based on normalized monthly climatic water balance, i.e. cumulative precipitation minus potential evapotranspiration (PET), summed over multiple time scales and computed as standard deviations with respect to long-term mean (Vicente-Serrano et al., 2010). The PET was here estimated with the Thornthwaite approach (Thornthwaite, 1948). The method requires surface temperature and latitude data only, and has therefore frequently been used for PET computations over the historical period. Moreover, the choice of methods is motivated by the larger confidence that is placed on GCM simulations of temperature compared to other

variables (vapor pressure, wind speed, net radiation, etc.) that are required for more physically based parameterizations of PET. At each grid point, model SPEI were derived from estimated PET and simulated rainfall over the past1000 and historical periods and then standardized against the 1901-2005 normalization period using the SPEI R package version 1.6 (Vicente-Serrano et al., 2010).

The proxy dataset was generated by a point-by-point regression (PPR) methodology that was applied to the TRW network to produce a SPEI reconstruction spanning the past millennium. The climate field reconstruction method is based on principal component regression procedure using the TRW chronologies as potential predictors to develop a set of nested multivariate stepwise regression models (see Cook et al., 1999 for details). Here we employed the same calibration/validation scheme, predictor selection and pre-processing steps as previously described in Seftigen et al. (2015). We performed a full period calibration over the 1901-1995 period of TRW/climate data overlap. A conventional split period calibration/validation procedure was additionally performed for an independent validation of the SPEI estimate, by splitting the full calibration period into two periods of roughly equal length (1901-1948 and 1949-1995 periods) and computing/comparing validation metrics over both periods. Each nest was centered and scaled to have the same mean and variance as the observational data in the calibration period. The instrumental SPEI target field for the reconstruction was computed from the CRU TS 3.22 (Harris et al., 2014) 0.5° latitude x 0.5° longitude gridded rainfall and temperature datasets over the southern portion of Scandinavia (55° - 65° N and 5° - 30° E) (Fig. 1), using the same conventions as described above. Simple correlation analysis conclusively demonstrated a short-term early summer moisture sensitivity of the TRW records over most of the study domain (Fig. S3). Based on these findings, we selected June SPEI, aggregated over a 2-month time scale, as the target season data for the reconstruction. A final regional time series was averaged from grid points where the calibration regression models explained at least 20% of instrumental variance and the reduction of error (RE) and coefficient of efficiency (CE) (National Research Council, 2006) verifications metrics exceeded the generally accepted threshold value of zero across all nests (N = 521 grid points). The mean tree-ring hydroclimate reconstruction (henceforth ScandH17) and the corresponding instrumental target dataset are shown in Fig. 1, and a validation of the reconstruction against 20th century instrumental data that have been withheld from the calibration is provided in supplementary materials (Fig. S4). Results are variable depending on the calibration/validation period used; the validation/calibration statistics are generally stronger for the 1901-1948 period and substantially weaker for the 1949-1995 period. The

most recent and well-replicated nests (mid-1600s to present) are generally explaining the greatest amount of instrumental variance (R^2 > 40% for the majority of the grid points). A loss of grid cells with declining proxy availability and a drop in reconstruction skill is occurring prior to the late-1400s and subsequently in the 1200s. Point-wise correlation with gridded instrumental SPEI dataset shows that ScandH17 is representative for a larger area in southern and central Scandinavia with a correlation 'hot spot' exceeding 0.6 (Fig. 1).

2.4. Analyses

The new proxy-based reconstruction was used to assess the temporal evolution of droughts and pluvials over the last millennium and to elucidate the mechanisms that govern hydroclimate changes in the northern European sector ranging from interannual to multidecadal time scales. We briefly analyze the relative role of temperature (which modulates potential evapotranspiration) and precipitation (which supplies moisture) in regional hydroclimate variability (sect. 5). We use the last-millennium and historical CMIP5/PMIP3 simulations of temperature and precipitation. As there are no independent, annually resolved, proxy reconstructions of rainfall variability currently available for the region, we only included temperature estimates in the analyses of ScandH17. For this purpose, the previously published Linderholm et al. (2014) (hereafter ScandT14) summer temperature reconstruction was used. The two reconstructions ScandH17 and ScandT14 share no common predictors and are thus fully independent, which ensures that any circular statement in the comparison can be ruled out. The ScandT14 record is based on tree-ring maximum density (MXD) and blue intensity data from central-northern Scandinavia and is in terms of signal strength and preserved multi-centennial scale variability one of the best temperature reconstructions currently available for the region.

Furthermore, we extended our analyses to the model domain using the methodology of paleoclimate data-model comparison. There were three main components to the combined approach. Firstly, we evaluated the consistency in various datasets and assessed whether the CMIP5/PMIP3 simulations have similar statistical properties as the reconstruction (sect. 3). Spectral and spectral coherency analyses were performed in two ways. The first is the multi-taper approach (Thomson, 1982) based on 4 tapers, where a Monte-Carlo procedure is used to estimate phase 95% confidence limits. We also used the wavelet cohere analyses available in the Grinsted et al. (2004) MATLAB package to assess the frequency dependent relationships and phasing between various datasets.

Secondly, we used the Superposed Epoch Analysis (SEA) (Haurwitz and Brier, 1981) to evaluate the influence of volcanic aerosol forcing on hydroclimate, temperature and precipitation of the Scandinavian region at inter-annual time scales (sect. 4). For the last millennium, monthly mean volcanic forcing series were obtained from three different sources: Gao et al. (2008), Crowley and Unterman (2013) and Sigl et al. (2015) datasets. We note that the former two forcings have been used as the boundary conditions for the last millennium CMIP5/PMIP3 simulations. The length of the proxy and model data allowed us to include sets of the 20 largest eruptions since 1100 CE (Table III) from the annual forcing series to assess the mean response. For each series and eruption, anomalies for ten post-eruption years were computed relative to a five-year pre-eruption mean. The confidence intervals around the composite responses were determined using a Monte Carlo block resampling (N = 10 000) of the actual event year windows (see Adams et al., 2003 for details).

Thirdly, we evaluated the skill of the models to represent the dynamics that drive the variability in hydroclimate of the Scandinavian region by establishing a link between simulated and reconstructed SPEI series and fields of mean sea level pressure (MSLP) over the Atlantic-European sector (sect. 5). Grid point correlations were computed to assess the spatial features and the strength of the teleconnections patterns over the modern era (1950-2005 CE). The analysis was also extended over the last millennium (1000-1849 CE) to investigate the nature of teleconnection stability without the influence of anthropogenic forcing. The gridded monthly instrumental HadSLP2 dataset spanning 1850-present (Allan and Ansell, 2006) was used for comparison with observed and proxy-based estimates of hydroclimate.

3. Modeled and reconstructed hydroclimate series

The regional warm season hydroclimate variability averaged across the six CMIP5/PMIP3 models together with the new ScandH17 proxy reconstruction over the last millennium are shown in Fig. 2a-b. Individual model SPEI time series are displayed in Fig. 2c-h. All data have been normalized and centred over the common interval from 1000 to 1995 CE, since this first joint proxy-model comparison focuses on the common relative changes rather than on the magnitude and the absolute values. A simple visual comparison reveals that the models and the reconstruction have generally little agreement in the variance structure and trends. The reconstruction is dominated by a large decadal-to-multidecadal variability while the multimodel mean is relatively flat at these time scales. There are some common features in some of the GCMs and the proxy datasets though (Fig. 2c-h), e.g., the drying in the 19th

296 century, but these are rare when the full millennium is considered and are likely occurring by
297 chance. The historical interval in the proxy record is characterized by a drought in the mid-
298 1800s and a gradual increase in wetness over the 20th century, while, with the exception of
299 short dry episode in the early-1900s, there is no long-term trend in the multimodel mean over
300 the modern era.

301 The very low correlation at inter-annual time scales is to be expected, as the internal
302 variations in the various records represent different realizations of the climate system, which
303 is to a very large extent chaotic at that time scale. The response of each ensemble member to a
304 strong external forcing applied to the model would nevertheless ideally agree (i.e. external
305 punctual perturbations such as volcanic eruptions could induce a coherent short-term
306 response, see sect. 4). Averaging across models or over multiple ensemble members will
307 reduce the contribution from stochastic variability so that the remaining signal can come
308 closer to the model response to external forcing. The comparison between ScandH17 and the
309 multimodel assemble mean reveal, however, no statistically significant agreement between
310 the series, neither on the interannual nor on decadal timescales, suggesting that the simulated
311 hydroclimate changes are not strongly tied to exogenous forcing. Moreover, we found no
312 statistically significant correlation between the different ensemble members in the same
313 model (CESM1) (Fig. 2c), which is the only model providing multiple ensemble members
314 (the only difference among these being the air temperature at the start of each ensemble
315 member (Otto-Bliesner et al., 2016) over the historical and past millennium intervals). The
316 poor overlap between CESM1 ensemble members as well as the individual GCM simulations
317 over the past millennium (despite the use of largely similar forcing series to drive the
318 simulations) is indicative of a larger contribution from internal variability on simulated
319 drought/pluvial occurrence than from changes in exogenous forcing.

320 We compare the spectral properties of the six individual CMIP5/PMIP3 models to
321 the ScandH17 reconstruction and observational data, which allows for a general evaluation of
322 potential frequency biases. Results indicate that the underlying spectrum of reconstructed
323 hydroclimate variability is significantly redder on decadal-centennial timescales than
324 indicated by the simulated SPEI (Fig. 3a and 3d), as has previously been noted (Ault et al.,
325 2012; Ault et al., 2013). In contrast, more hydroclimate variance is concentrated on
326 interannual timescales in the CMIP5/PMIP3 archive than in ScandH17 reconstruction. At
327 frequency bands < 8 years, the power spectral range of most models is systematically above
328 the confidence interval of ScandH17. We also consider the agreement between simulated,
329 reconstructed (ScandT14) and instrumental temperature data in terms of their spectral

properties (Fig. 3b). Although the degree of agreement is higher than for hydroclimatology and most models lie within the reconstruction confidence bands (see also sect. S2 supplementary materials), there are some models that have more variance than the reconstruction at periods < 10 years.

4. The role of volcanic forcing

Large explosive volcanic eruptions are an important natural radiative forcing mechanism at timescales ranging from seasons to decades (Shindell et al., 2004; Gleckler et al., 2006). The imposed perturbation on the climate system by such events will depend on the nature of the eruption, the magnitude of change in the energy entering the earth's atmosphere, the background climate and internal variability, latitude and season. Analysis of observational data (Shindell et al., 2004), tree-ring records (D'Arrigo et al., 2013) and model simulations (Anchukaitis et al., 2010) indicate a considerable spatial variability in the dynamical response of the climate system to volcanic forcing, with some regions experience surface and tropospheric cooling effects and other regions showing no significant change or even warming effect. Here, we assess the magnitude and timing of Scandinavian summer temperature, rainfall and hydroclimate response to short-term radiative cooling due to volcanic aerosols.

A peak cooling is observed one year after the eruption, both in ScandT14 and in the CMIP5/PMIP3 composite average, for all the three forcings considered (Fig. 4). In addition, there is a significant cooling in the year of the event for the Crowley and Unterman (2013) and Sigl et al. (2015) lists. ScandT14 reveal a marginally greater cooling (2.0 °C, mean of the three event lists) than the model average (1.8 °C) one year after the eruption. Remarkably, there is a high degree of similarity in the proxy and in the GCMs not only in terms of the signal timing and the magnitude of the cooling response, but also the rate of recovery. A complete recovery after the volcanic cooling is found two years after the eruption, independent of the forcing list. These results are generally consistent with prior studies (Fischer et al., 2007; Jones et al., 2013; McCarroll et al., 2013) highlighting the importance of explosive volcanism as an external driver of Northern European temperature variability. They also provide a relevant test of the model to radiation perturbations. The agreement between the model simulations and proxy data demonstrates the credibility of the models.

Existing research on the response of high-latitude rainfall and hydroclimate to volcanism is limited (in part because high resolution moisture sensitive proxy records are sparse or unavailable). Fischer et al. (2007) found a weak tendency to drying conditions over

southern/central Scandinavia in the summer of year 0 and year 1 after the eruption. Circulation changes to the surface cooling were shown to modulate the directly forced response. On continental and global scales, both observational and modeling studies have found a decrease in precipitation (Iles et al., 2013) and streamflow (Iles and Hegerl, 2015) in response to large explosive eruptions, particularly in climatologically humid regions (Carley and Gabriele, 2014). The short-term drying is caused by a reduction in incoming solar radiation reaching the surface, which reduces evaporation, whilst the widespread cooling stabilized the atmosphere and lowers its water holding capacity (Bala et al., 2008). Here, we apply SEA on ScandH17 and simulated SPEI and precipitation to examine the influence of volcanism on Scandinavian moisture availability. A statistically significant reduction in simulated rainfall is observed for all event lists, ranging between the year of the event (Crowley and Unterman, 2013 dataset) and up to two years (Sigl et al., 2015 dataset) following the eruption. We find, however, that the precipitation signal is less consistent across the six CMIP5/PMIP3 models than the cooling effect observed in the simulated temperature series.

The SEA on SPEI time series reveals a statistically significant drying after large volcanism. However, the response is more muted than the response of temperature and rainfall separately. Moreover, the agreement between proxy data and the model composite average is weak and there are large inconsistencies between the different forcing records. ScandH17 show a progressive transition from wet conditions in the event year and preceding years to dryer conditions in the consecutive years with significant dry anomalies five (Crowley and Unterman, 2013 dataset) and seven years (Sigl et al., 2015; Gao et al., 2008 datasets) after the perturbation. For the CMIP5/PMIP3 multimodel multi-eruption average, only the fifth year after the eruption (Crowley and Unterman, 2013 list) is found to be significantly drier than the adjacent years.

The observed weak influence of volcanic forcing on the hydroclimate of the region can be explained by various factors. For example, our results reveal that GCM simulated post-volcanic cooling remains significant for about two years and matches the timescale of the post-volcanic rainfall decrease. Since the SPEI accounts for both supply and demand changes, the net effect would be such that the temperature-driven PET decrease counter a substantial fraction of the precipitation-driven drying, thus producing SPEI values near neutral. Furthermore, the muted response of ScandH17 may arise from autocorrelated biological memory in the TRW data (Esper et al., 2015). The high year-to-year persistence may bias its ability to estimate the abruptness and severity of climatic extremes caused by volcanic

cooling. The tree-ring MXD and the blue intensity parameters have, in contrast, been suggested to be superior to TRW for recording short term climate perturbations (Wilson et al., 2016), which is likely the reason why the response of ScandT14 is more immediate than that of ScandH17.

5. Internal sources of variability

If the regional hydroclimate variability is indeed dominated by internally generated stochastic components of variability (see sect. 3), atmospheric circulation changes can be the key process shaping regional patterns of moisture availability. Advancing our understanding of the range, stability and strength of teleconnection behavior (defined here as the correlation between hydroclimate and MSLP over the Atlantic-European sector) and its coupling to regional hydroclimate would provide an improved understanding of drought/pluvial dynamics and associated uncertainty. In this section, we first explore major modes of atmosphere variability that impact summertime northern European hydroclimatology. We also assess more extensively the contribution of atmospheric processes (and possible land-atmosphere interactions) by investigating the couplings between hydroclimate and arguably the two most critical variables of the terrestrial climate and the hydrological cycle: precipitation and temperature.

To determine the role of teleconnections, correlation of MSLP fields with the hydroclimatic variables over the recent 50 years of the post-industrial era were computed. Results are shown in Fig. 5. As expected, we find that atmospheric dynamics have a significant role in climate variability in the region: a strong correlation with regional hydroclimate is found when MSLP in concurrent months (i.e. May-June) is considered. The results show that the proxy based and CMIP5/PMIP3 simulated dynamics are largely consistent with those in the instrumental record, indicating that both the proxy and the models contain to some degree realistic teleconnections. A consistent feature across the datasets is a tripole structure that would favor increased moisture supply into the Scandinavian region. The structure is characterized by anomalous cyclonic conditions across Scandinavia and high-pressure systems extending over Iceland-Greenland and, albeit less pronounced, over European Russia - Central Asia. Out of the six CMIP5/PMIP3 models, MIROC-ESM is the one showing the largest discrepancy with the major spatial features of the observed correlation map, by failing to reproduce the anti-cyclonic pattern over Iceland-Greenland. Additionally, MIROC-ESM and also CCSM4 show a meridional and zonal shift of the European Russia - Central Asia high-pressure structure towards the Mediterranean region.

Atmospheric circulation has been identified as key contributor to recent changes in the climate of Europe in both summer and winter (van Oldenborgh and Van Ulden, 2003; Jones and Lister, 2009). To assess the stationarity of observed MSLP patterns, the analysis was repeated for the pre-industrial last millennium (1000-1849 CE) period (Fig. 6). The exercise was restricted to five GCMs for which simulated MSLP was available for the pre-industrial era (BCC-CSM1-1 was not included). The simulated dynamical relationships were found to be largely stable for all five models, being consistent with observed correlations patterns in the modern era. This suggests a weak influence of anthropogenic forcing on the structure of the dynamical drivers of Scandinavian hydroclimate. In addition to raw data, correlation analysis with 10-year low-passed data was also completed for the pre-industrial period with the purpose to elucidate the drivers of multidecadal hydroclimate variability. We find similar, yet weaker, correlation patterns as compared to the high-frequency variations (results not shown).

Precipitation and temperature are the two key variables of the hydrological cycle. Assessing the relative contribution of these two variables to the surface moisture balance across various timescales, and the mechanisms that control and modulate it, is therefore of great interest to the study of regional processes on surface energy and water budgets. While past studies have investigated the relationship between temperature, moisture supply and drought in various regions on daily, seasonal and interannual timescales (Adler et al., 2008; Berg et al., 2015; Trenberth, 2011; Madden and Williams, 1978), the nature of concurrent multidecadal/ long-term relationship is still far from being clear. A join analyses of the new hydroclimate reconstruction with the recently published Linderholm et al. (2014- ScandT14) fully independent warm-season temperature record for Scandinavia is provided in Figs. 7 and 8, in conjunction with the CMIP5/PMIP3 simulations of temperature, rainfall and SPEI. On interannual timescales, five out of six GCMs show a significant ($p < 0.05$) negative association between simulated interannual temperature and rainfall, with correlation coefficients ranging between $r = -0.12$ and -0.29 (1000-2005 CE period). Moreover, all model show a strong negative (positive) correlation between temperature (precipitation) and SPEI in the last millennium, ranging between $r = -0.63$ and -0.80 ($r = 0.61$ and 0.84). Extending the analysis to the instrumental data, we find that the regional year-to-year variability in hydroclimate is more closely organized around changes in precipitation than changes in temperature (Fig. S5). In southern Scandinavia, weak negative correlations appear between temperature and rainfall (Fig. S5a), and temperature and SPEI (Fig. S5b). Over northern Scandinavia, the interannual correlations are not significant.

Turning to the tree-ring records, we find no significant relationship between ScandH17 and ScandT14 reconstructions on a year-to-year basis ($r = 0.01$ and $p = 0.8$ on first difference data, 1100-1995 CE period). The considerable distance separating the sampling sites of each tree-ring collection, and the fact that summer precipitation occurrence often depends on local processes and moisture fluxes could explain the lack of a shared annual signal. Notably, however, we find that the two reconstructions are mostly in phase on decadal and longer timescales ($r = 0.30$ and $p < 0.001$ on loess-smoothed data, 1100-1995 CE period) (Fig. 7), suggesting that the low-frequency temperature and hydroclimate variability is more spatially coherent. These results are corroborated by the cross-wavelet coherency analysis (Fig. 8a), revealing that the ScandH17 and ScandT14 reconstructions share significant ($p < 0.05$) in phase variance in multidecadal frequency throughout most of the last millennium. The coupling seems to arise from overlap in shared frequencies at wavelengths longer than ~ 50 years (c.f. Fig. 3). Interestingly, we find that the paleoclimatic evidence and the CMIP5/PMIP3 models portray a considerably different response of hydroclimate in Scandinavia to long-term temperature changes. While the proxy time series suggests that prolonged wet periods generally coincide with elevated temperatures, the majority of the CMIP5/PMIP3 models indicate that warm decades should have been dryer (Fig. 8b – h and Fig. S9).

Instrumental and paleoclimate evidence collectively suggest a time-dependent shift of the relationship between regional temperature and hydroclimate, which in turn implies that different mechanisms governing the climate system might be operating at high (interannual) and low (decadal/longer) frequencies, respectively. The previously discussed strong link between inter-annual regional hydroclimate variability and atmospheric pressure patterns indicates that atmospheric dynamics is likely a dominant driver of hydroclimate in the northern European sector on interannual basis. The inverse covariability between warm-season temperature and moisture supply, which is revealed by the instrumental record, may arise from synoptic-scale correspondence between reduced cloud cover/rainfall and increased incoming shortwave radiation warming the surface during clear sky conditions. In addition, soil moisture exert a strong influence on the allocation of available energy between latent and sensible heating, especially in the warm-season (Seneviratne et al., 2010). Reduced soil moisture, for example, is associated with reduced latent heat flux and thus increased sensible heating and higher air temperatures near the surface. Resulting positive feedbacks of a modified surface heat flux partitioning on cloud cover and radiation (Gentine et al., 2013) and

large-scale circulation (Haarsma et al., 2009) could further strengthen the influence of rainfall variability on the thermal climate.

The positive association between temperature and SPEI that is found in the proxy records on decadal-to-multidecadal timescales could imply that the long-term regional hydroclimate variability is more sensitive to changes in moisture supply (precipitation) rather than to increased evaporative demand due to warming. It may also suggests that the regional moisture balance might be favored by the Clausius-Clapeyron relation (Allen and Ingram, 2002), prescribing an increase in rainfall and intensity of the hydrological cycle during warmer periods in the past millennium. This is generally referred to as 'wet-get-wetter'/'dry-get-dryer' mechanism and is attributed to thermodynamics processes (Held and Soden, 2006). In the absence of changes in atmospheric circulation, changes in net moisture supply with warming are related to change in moisture content of the atmosphere. It presupposes that existing circulations will transport more moisture into mesic regions of the globe (e.g., tropics and the mid- to latitudes of Northern Hemisphere), whilst dry regions (e.g., subtropics) will get even dryer, with the fractional change determined by Clausius-Clapeyron relation. In contrast to the proxy records, the model composite average reveals a twentieth-century temperature and rainfall increase yet little change in hydroclimate (Fig. 7b). The multimodel assessment implies that natural variability plays only a subsidiary role in recent changes and that forcing from anthropogenic greenhouse gases (GHG) may have played a more important role (as previously discussed, the effect of GHG-forcing on interannual teleconnection patterns in the modern era seems to be weak). Moreover, the absences of any significant trend in simulated SPEI series indicates that the gains in moisture from increased precipitation are large enough to compensate for any GHG-induced increase in PET in the post-industrial period.

6. Summary and discussion

This study presents the first comprehensive assessment of past variability and trends in hydroclimate of northern European sector over the last millennium of the Common Era along with interrelated variables: precipitation, which supplies moisture, and temperature, which modulates evapotranspiration. A combined approach comparing observational (both instrumental and proxy based) and model-based results is used for evaluation of simulated and real-world interannual-to-centennial climate variability and the underlying physics governing the climate system. A number of important finding emerge from the collective comparison:

[1] Models and proxy data are found to broadly agree on the modes of atmospheric variability (sect. 5) that produces droughts and pluvials in Scandinavia. Despite these dynamical similarities, large discrepancies between model simulations and the proxy reconstruction are shown to exist. The droughts and pluvials in the forced simulation are not temporally synchronous with those in the proxy record, nor do the GCM spectra agree with the proxy spectra on the amount of variance present on short and long timescales (sect. 3).

[2] The proxy data and the CMIP5/PMIP3 models reveal different effects of long-term temperature changes on summer hydroclimate in Scandinavia. According to the GCMs, prolonged droughts generally coincide with elevated temperatures. The proxy evidence, on the other hand, suggests that warm decades in the last millennium also tend to be wet decades. Although the precise reason for the model-proxy mismatch remains to be unraveled, our results suggests that spectral inconsistencies among the model and proxy datasets could be one possible explanation for the mismatch.

[3] There are considerable disagreements among hydroclimate features shown by the CMIP5/PMIP3 simulations (despite the use of largely similar forcing series) (sect. 3). Together, these results point to the possibilities of dominant influence of stochastic processes for the regional hydroclimate and/or deficiencies in the models to realistically represent relevant processes in reality.

Most notably we find clear inconsistencies between the paleoclimate record and the model spectra. At multidecadal/longer timescale there is more variability in the proxy data than in the models. In contrast, the dominance of GCM simulated interannual components of variability is not reflected in the proxy record. It is difficult to determine explicitly whether it is an external forcing or internal sources that drive the decadal and longer variance in the proxy reconstruction. Prior studies have highlighted the importance of external influences on regional climate variability at different timescales (e.g., Gleckler et al., 2006; Thiéblemont et al., 2015; Sigl et al., 2015). Although we find a short term response of regional hydroclimate to volcanic perturbations (sect. 4), multi-year anomalies in the proxy reconstruction do, however, not appear to correspond well with the epochs following the large volcanic eruptions (e.g., in the 1250s, 1450s and 1810s) used to force the models. Thus we cannot rule out that the variability in the reconstruction largely arise from internal sources of variation. Consequently, if the proxy-inferred decadal-to-multidecadal variability is accurate and if the variability is indeed largely unforced, then its magnitude is well beyond what any of the current generation global climate models are able to produce in the region. Underestimation of redness in the models on multidecadal/longer timescales, suggests the GCMs might be

lacking/underestimating processes important to the variability at these timescales. There are a number of recognized limitations relating to the dynamics that are relevant to the climatology of the North Atlantic-European sectors. One such example is that models have generally been unable to simulate low-frequency variability in the North Atlantic Oscillation (Osborn, 2004). They have also been shown to underestimate the periodicity of the Atlantic Multidecadal Oscillation (Kavvada et al., 2013), which has implications for the associated hydroclimate impact on neighboring continents (Coats et al., 2015). If, on the other hand, the proxy estimated multidecadal/longer variability in the last millennium is forced by exogenous mechanisms, then either 1) it is a forcing component that is largely missing in the CMIP5/PMIP3 models, alternatively, 2) it is a forcing component that generates a different long-term response in the models compared to the "proxy view" of regional hydroclimatology.

It is not possible to pinpoint which part of the disagreement between models and the proxy comes from uncertainties in the tree-ring reconstruction, deficiencies in the forcing series used to drive the models, or from deficiencies in the model. Our analyses have included precipitation simulation – a challenging variable for GCMs to simulate accurately. The coarse spatial resolution of the models gives only an approximate representation of the topographic features, which are important for regional hydroclimate. Another possibility is that the scale of the GCMs is unrepresentative of the point estimate provided by the ScandH17 reconstruction. On the other hand, the mismatch between grid box and point estimates is expected to reduce at longer timescales (Jones et al., 1997). There are also limitations of the tree-ring proxy and uncertainties in the interpretation of the data that cannot be ignored. Tree-rings and other biological archives may integrate climate conditions over multiple years (Zhang et al., 2015), which could potentially overestimating the ratio of low to high frequency variability (Franke et al., 2013). While we have been able to establish that prevailing summer moisture availability has been the main growth limitation of trees in the ScandH17 network on an interannual basis over the twentieth century (Figs. S3 and S6), we cannot verify the drought-tree growth model in the pre-instrumental era or across longer spectrum of variability. We are not able to rule out that there might have been climatic regimes in the past that would have caused dynamical shift in the tree growth response to climate, and potentially have called into question the uniformitarian paradigm traditionally applied in the field of dendroclimatology. These non-stationaries may include frequency dependent sensitivity of the proxy system to climate. While we are able to show that the year-to-year variability of growth is dominated by a moisture signal, the impact of growing season temperature on lower

598 frequency variations has yet to be established. In addition to these issues, there are also risks
599 that less well know dynamics outside the climate system may introduce variability into the
600 records at decadal/longer timescales. Advances in the mechanistic understanding of the
601 various proxies and the processes through which they record environmental change, e.g.,
602 through development and refinement of process-based forward models (Tolwinski-Ward et
603 al., 2011), is currently an emerging priority in the field.

604 The discrepancies in CMIP5/PMIP3 simulated and proxy reconstructed hydroclimate
605 variability in the last millennium is an issue that must be addressed when assessing
606 projections of future hydroclimate change. The lack of adequate understanding for
607 mechanisms linking temperature and moisture supply on longer timescales has important
608 implication for future projections. Weak multidecadal variability in models also implies that
609 inference about future persistent droughts and pluvials based on the latest generation global
610 climate models will likely underestimate the true risk of these events. Reconciliations for the
611 apparent proxy – model mismatch will require efforts from the proxy, modeling and statistics
612 groups, including additional proxy records and refined model simulations of hydroclimate
613 variability in the last millennium, together with the development of alternative approaches for
614 joint proxy-model assessments. Having here provided a first comparison of reconstructed and
615 simulated hydroclimate for Scandinavia, our future efforts will include adaptions of the data
616 assimilation approach to paleoclimate reconstruction. Such efforts hold promise for reducing
617 the uncertainties associated with model physics, external forcings, and internal climate
618 variability, and ultimately help to refine our view of past and future hydroclimate changes.

619 **Data availability**

620 The raw tree-ring data can be downloaded from the International Tree-Ring Data Bank
621 (http://www.ncdc.noaa.gov/paleo/treering.html) and the SAIMA Tree-Ring Data Bank
622 (http://lustiag.pp.fi/Saima/dendrotieto.htm) (Table II). The CMIP5/PMIP3 climate model
623 output can be obtained though the Earth System Grid - Center for Enabling Technologies
624 (ESG-CET) portal (http://pcmdi9.llnl.gov/). The ScandT14 temperature reconstruction is
625 archived through the NOAA paleoclimate database (citation added on publication). The
626 ScandH17 reconstruction and standardized tree-ring chronologies are provided in the
627 supporting information.

628 **Acknowledgments**

K. Seftigen was supported by the FORMAS mobility starting grant for young researchers (grant # 2014-723). H. Goosse is senior research associate with the FRS/FNRS, Belgium. The authors wish to acknowledge the World Climate Research Programme's Working Group on Coupled Modelling, which is responsible for CMIP, and to thank the climate modeling groups (listed in Table I of this paper) for producing and making available their model output. For CMIP the U.S. Department of Energy's Program for Climate Model Diagnosis and Intercomparison provides coordinating support and led development of software infrastructure in partnership with the Global Organization for Earth System Science Portals. The authors also wish to acknowledge the researchers who have produced and made their tree-ring chronologies available.

References

Adams, B. J., Mann, M. E., and Ammann, C. M.: Proxy evidence for an El Nino-like response to volcanic forcing, Nature, 426, 274-278, 2003.

Adler, R. F., Gu, G., Wang, J.-J., Huffman, G. J., Curtis, S., and Bolvin, D.: Relationships between global precipitation and surface temperature on interannual and longer timescales (1979–2006), Journal of Geophysical Research, 113, 10.1029/2008jd010536, 2008.

Allan, R., and Ansell, T.: A New Globally Complete Monthly Historical Gridded Mean Sea Level Pressure Dataset (HadSLP2): 1850–2004, Journal of Climate, 19, 5816-5842, 10.1175/jcli3937.1, 2006.

Allen, M. R., and Ingram, W. J.: Constraints on future changes in climate and the hydrologic cycle, Nature, 419, 224-232, 2002.

Anchukaitis, K. J., Buckley, B. M., Cook, E. R., Cook, B. I., D'Arrigo, R. D., and Ammann, C. M.: Influence of volcanic eruptions on the climate of the Asian monsoon region, Geophysical Research Letters, 37, n/a-n/a, 10.1029/2010gl044843, 2010.

Ault, T. R., Cole, J. E., and St. George, S.: The amplitude of decadal to multidecadal variability in precipitation simulated by state-of-the-art climate models, Geophysical Research Letters, 39, n/a-n/a, 10.1029/2012gl053424, 2012.

Ault, T. R., Cole, J. E., Overpeck, J. T., Pederson, G. T., St. George, S., Otto-Bliesner, B., Woodhouse, C. A., and Deser, C.: The Continuum of Hydroclimate Variability in Western North America during the Last Millennium, Journal of Climate, 26, 5863-5878, 10.1175/jcli-d-11-00732.1, 2013.

Bala, G., Duffy, P. B., and Taylor, K. E.: Impact of geoengineering schemes on the global hydrological cycle, Proceedings of the National Academy of Sciences, 105, 7664-7669, 10.1073/pnas.0711648105, 2008.

Berg, A., Lintner, B. R., Findell, K., Seneviratne, S. I., van den Hurk, B., Ducharne, A., Chéruy, F., Hagemann, S., Lawrence, D. M., Malyshev, S., Meier, A., and Gentine, P.: Interannual Coupling between Summertime Surface Temperature and Precipitation over Land: Processes and Implications for Climate Change*, Journal of Climate, 28, 1308-1328, 10.1175/jcli-d-14-00324.1, 2015.

Björklund, J., Gunnarson, B. E., Krusic, P. J., Grudd, H., Josefsson, T., Östlund, L., and Linderholm, H. W.: Advances towards improved low-frequency tree-ring reconstructions, using an updated Pinus sylvestris L. MXD network from the Scandinavian Mountains, Theor Appl Climatol, 10.1007/s00704-012-0787-7, 2012.

Björklund, J., Gunnarson, B. E., Seftigen, K., Esper, J., and Linderholm, H. W.: Blue intensity and density from northern Fennoscandian tree rings, exploring the potential to improve summer temperature reconstructions with earlywood information, Climate of the Past, 10, 877-885, 10.5194/cp-10-877-2014, 2014.

675 Briffa, K. R., Jones, P. D., Bartholin, T. S., Eckstein, D., Schweingruber, F. H., Karlén, W.,
676 Zetterberg, P., and Eronen, M.: Fennoscandian summers from ad 500: temperature changes on short
677 and long timescales, Climate Dynamics, 7, 111-119, 10.1007/bf00211153, 1992.
678 Briffa, K. R., and Melvin, T. M.: A Closer Look at Regional Curve Standardization of Tree-Ring
679 Records: Justification of the Need, a Warning of Some Pitfalls, and Suggested Improvements in Its
680 Application, in: Dendroclimatology: Progress and Prospects, edited by: Hughes, M. K., Swetnam, T.
681 W., and Diaz, H. F., Springer Netherlands, Dordrecht, 113-145, 2011.
682 Carley, E. I., and Gabriele, C. H.: The global precipitation response to volcanic eruptions in the
683 CMIP5 models, Environmental Research Letters, 9, 104012, 2014.
684 Coats, S., Cook, B. I., Smerdon, J. E., and Seager, R.: North American Pancontinental Droughts in
685 Model Simulations of the Last Millennium*, Journal of Climate, 28, 2025-2043, 10.1175/jcli-d-14-
686 00634.1, 2015.
687 Cook, E. R., Briffa, K. R., Meko, D., Graybill, D. A., and Funkhouser, G.: The 'segment length curse'
688 in long tree-ring chronology development for palaeoclimatic studies, The Holocene, 5, 229-237, 1995.
689 Cook, E. R., Meko, D. M., Stahle, D. W., and Cleaveland, M. K.: Drought Reconstructions for the
690 Continental United States, Journal of Climate, 12, 1145-1162, 1999.
691 Cook, E. R., and Krusic, P. J.: Arstan, version 2005, Tree-ring labora- tory, Lamont-Doherty Earth
692 Obs., Palisades, N. Y. (Available at http://www.ldeo.columbia.edu/trl), 2005.
693 Cook, E. R., Seager, R., Kushnir, Y., Briffa, K. R., Büntgen, U., Frank, D., Krusic, P. J., Tegel, W.,
694 van der Schrier, G., Andreu-Hayles, L., Baillie, M., Baittinger, C., Bleicher, N., Bonde, N., Brown, D.,
695 Carrer, M., Cooper, R., Čufar, K., Dittmar, C., Esper, J., Griggs, C., Gunnarson, B., Günther, B.,
696 Gutierrez, E., Haneca, K., Helama, S., Herzig, F., Heussner, K.-U., Hofmann, J., Janda, P., Kontic, R.,
697 Köse, N., Kyncl, T., Levanič, T., Linderholm, H., Manning, S., Melvin, T. M., Miles, D., Neuwirth,
698 B., Nicolussi, K., Nola, P., Panayotov, M., Popa, I., Rothe, A., Seftigen, K., Seim, A., Svarva, H.,
699 Svoboda, M., Thun, T., Timonen, M., Touchan, R., Trotsiuk, V., Trouet, V., Walder, F., Ważny, T.,
700 Wilson, R., and Zang, C.: Old World megadroughts and pluvials during the Common Era, Science
701 Advances, 1, 10.1126/sciadv.1500561, 2015.
702 Crowley, T. J., and Unterman, M. B.: Technical details concerning development of a 1200 yr proxy
703 index for global volcanism, Earth Syst. Sci. Data, 5, 187-197, 10.5194/essd-5-187-2013, 2013.
704 D'Arrigo, R., Wilson, R., and Anchukaitis, K. J.: Volcanic cooling signal in tree ring temperature
705 records for the past millennium, Journal of Geophysical Research: Atmospheres, 118, 9000-9010,
706 10.1002/jgrd.50692, 2013.
707 Drobyshev, I., Niklasson, M., Linderholm, H. W., Seftigen, K., Hickler, T., and Eggertsson, O.:
708 Reconstruction of a regional drought index in southern Sweden since AD 1750, The Holocene, 21,
709 667-679, 10.1177/0959683610391312, 2011.
710 Dufresne, J. L., Foujols, M. A., Denvil, S., Caubel, A., Marti, O., Aumont, O., Balkanski, Y., Bekki,
711 S., Bellenger, H., Benshila, R., Bony, S., Bopp, L., Braconnot, P., Brockmann, P., Cadule, P., Cheruy,
712 F., Codron, F., Cozic, A., Cugnet, D., de Noblet, N., Duvel, J. P., Ethé, C., Fairhead, L., Fichefet, T.,
713 Flavoni, S., Friedlingstein, P., Grandpeix, J. Y., Guez, L., Guilyardi, E., Hauglustaine, D., Hourdin, F.,
714 Idelkadi, A., Ghattas, J., Joussaume, S., Kageyama, M., Krinner, G., Labetoulle, S., Lahellec, A.,
715 Lefebvre, M. P., Lefevre, F., Levy, C., Li, Z. X., Lloyd, J., Lott, F., Madec, G., Mancip, M.,
716 Marchand, M., Masson, S., Meurdesoif, Y., Mignot, J., Musat, I., Parouty, S., Polcher, J., Rio, C.,
717 Schulz, M., Swingedouw, D., Szopa, S., Talandier, C., Terray, P., Viovy, N., and Vuichard, N.:
718 Climate change projections using the IPSL-CM5 Earth System Model: from CMIP3 to CMIP5,
719 Climate Dynamics, 40, 2123-2165, 10.1007/s00382-012-1636-1, 2013.
720 Esper, J., Frank, D. C., Timonen, M., Zorita, E., Wilson, R. J. S., Luterbacher, J., Holzkamper, S.,
721 Fischer, N., Wagner, S., Nievergelt, D., Verstege, A., and Buntgen, U.: Orbital forcing of tree-ring
722 data, Nature Clim. Change, 2, 862-866, 2012.
723 Esper, J., Schneider, L., Smerdon, J. E., Schöne, B. R., and Büntgen, U.: Signals and memory in tree-
724 ring width and density data, Dendrochronologia, 35, 62-70,
725 http://dx.doi.org/10.1016/j.dendro.2015.07.001, 2015.
726 Feng, S., Hu, Q., and Oglesby, R. J.: Influence of Atlantic sea surface temperatures on persistent
727 drought in North America, Climate Dynamics, 37, 569-586, 10.1007/s00382-010-0835-x, 2011.

Fischer, E. M., Luterbacher, J., Zorita, E., Tett, S. F. B., Casty, C., and Wanner, H.: European climate response to tropical volcanic eruptions over the last half millennium, Geophysical Research Letters, 34, n/a-n/a, 10.1029/2006GL027992, 2007.
Frank, D. C., Esper, J., and Cook, E. R.: On variance adjustments in tree-ring chronology development, Tree rings in archaeology, climatology and ecology, TRACE, 4, 56-66, 2006.
Franke, J., Frank, D., Raible, C. C., Esper, J., and Bronnimann, S.: Spectral biases in tree-ring climate proxies, Nature Clim. Change, 3, 360-364, 2013.
Gao, C., Robock, A., and Ammann, C.: Volcanic forcing of climate over the past 1500 years: An improved ice core-based index for climate models, Journal of Geophysical Research: Atmospheres, 113, n/a-n/a, 10.1029/2008JD010239, 2008.
Gentine, P., Holtslag, A. A. M., D'Andrea, F., and Ek, M.: Surface and Atmospheric Controls on the Onset of Moist Convection over Land, Journal of Hydrometeorology, 14, 1443-1462, 10.1175/jhm-d-12-0137.1, 2013.
Gleckler, P. J., Wigley, T. M. L., Santer, B. D., Gregory, J. M., AchutaRao, K., and Taylor, K. E.: Volcanoes and climate: Krakatoa's signature persists in the ocean, Nature, 439, 675-675, 2006.
Grinsted, A., Moore, J. C., and Jevrejeva, S.: Application of the cross wavelet transform and wavelet coherence to geophysical time series, Nonlin. Processes Geophys., 11, 561-566, 10.5194/npg-11-561-2004, 2004.
Gunnarson, B. E., Linderholm, H. W., and Moberg, A.: Improving a tree-ring reconstruction from west-central Scandinavia: 900 years of warm-season temperatures, Climate Dynamics, 36, 97-108, 10.1007/s00382-010-0783-5, 2011.
Haarsma, R. J., Selten, F., Hurk, B. v., Hazeleger, W., and Wang, X.: Drier Mediterranean soils due to greenhouse warming bring easterly winds over summertime central Europe, Geophysical Research Letters, 36, n/a-n/a, 10.1029/2008GL036617, 2009.
Harris, I., Jones, P. D., Osborn, T. J., and Lister, D. H.: Updated high-resolution grids of monthly climatic observations – the CRU TS3.10 Dataset, International Journal of Climatology, 34, 623-642, 10.1002/joc.3711, 2014.
Haurwitz, M. W., and Brier, G. W.: A Critique of the Superposed Epoch Analysis Method: Its Application to Solar–Weather Relations, Monthly Weather Review, 109, 2074-2079, 10.1175/1520-0493(1981)109<2074:acotse>2.0.co;2, 1981.
Hegerl, G. C., Black, E., Allan, R. P., Ingram, W. J., Polson, D., Trenberth, K. E., Chadwick, R. S., Arkin, P. A., Sarojini, B. B., Becker, A., Dai, A., Durack, P. J., Easterling, D., Fowler, H. J., Kendon, E. J., Huffman, G. J., Liu, C., Marsh, R., New, M., Osborn, T. J., Skliris, N., Stott, P. A., Vidale, P.-L., Wijffels, S. E., Wilcox, L. J., Willett, K. M., and Zhang, X.: Challenges in Quantifying Changes in the Global Water Cycle, Bulletin of the American Meteorological Society, 96, 1097-1115, 10.1175/bams-d-13-00212.1, 2015.
Helama, S., and Lindholm, M.: Droughts and rainfall in south eastern Finland since AD 874, inferred from Scots pine tree-rings, Boreal Environ Res, 8, 171-183, 2003.
Helama, S., Merilainen, J., and Tuomenvirta, H.: Multicentennial megadrought in northern Europe coincided with a global El Nino-Southern Oscillation drought pattern during the Medieval Climate Anomaly, Geology, 37, 175-178, 10.1130/g25329a.1, 2009.
Held, I. M., and Soden, B. J.: Robust Responses of the Hydrological Cycle to Global Warming, Journal of Climate, 19, 5686-5699, 10.1175/jcli3990.1, 2006.
Iles, C. E., Hegerl, G. C., Schurer, A. P., and Zhang, X.: The effect of volcanic eruptions on global precipitation, Journal of Geophysical Research: Atmospheres, 118, 8770-8786, 10.1002/jgrd.50678, 2013.
Iles, C. E., and Hegerl, G. C.: Systematic change in global patterns of streamflow following volcanic eruptions, Nature Geoscience, 8, 838-842, 10.1038/ngeo2545, 2015.
Jones, P. D., Osborn, T. J., and Briffa, K. R.: Estimating Sampling Errors in Large-Scale Temperature Averages, Journal of Climate, 10, 2548-2568, 10.1175/1520-0442(1997)010<2548:eseils>2.0.co;2, 1997.
Jones, P. D., and Lister, D. H.: The influence of the circulation on surface temperature and precipitation patterns over Europe, Clim. Past, 5, 259-267, 10.5194/cp-5-259-2009, 2009.

781 Jones, P. D., Melvin, T. M., Harpham, C., Grudd, H., and Helama, S.: Cool North European summers
782 and possible links to explosive volcanic eruptions, Journal of Geophysical Research: Atmospheres,
783 118, 6259-6265, 10.1002/jgrd.50513, 2013.
784 Jönsson, K., and Nilsson, C.: Scots Pine (pinus sylvestrisL.) on Shingle Fields: A Dendrochronologic
785 Reconstruction of Early Summer Precipitation in Mideast Sweden, Journal of Climate, 22, 4710-4722,
786 10.1175/2009jcli2401.1, 2009.
787 Jungclaus, J. H., Lohmann, K., and Zanchettin, D.: Enhanced 20th-century heat transfer to the Arctic
788 simulated in the context of climate variations over the last millennium, Clim. Past, 10, 2201-2213,
789 10.5194/cp-10-2201-2014, 2014.
790 Kavvada, A., Ruiz-Barradas, A., and Nigam, S.: AMO's structure and climate footprint in
791 observations and IPCC AR5 climate simulations, Climate Dynamics, 41, 1345-1364, 10.1007/s00382-
792 013-1712-1, 2013.
793 Landrum, L., Otto-Bliesner, B. L., Wahl, E. R., Conley, A., Lawrence, P. J., Rosenbloom, N., and
794 Teng, H.: Last Millennium Climate and Its Variability in CCSM4, Journal of Climate, 26, 1085-1111,
795 10.1175/JCLI-D-11-00326.1, 2012.
796 Lehner, F., Joos, F., Raible, C. C., Mignot, J., Born, A., Keller, K. M., and Stocker, T. F.: Climate and
797 carbon cycle dynamics in a CESM simulation from 850 to 2100 CE, Earth Syst. Dynam., 6, 411-434,
798 10.5194/esd-6-411-2015, 2015.
799 Linderholm, H., and Molin, T.: Early nineteenth century drought in east central Sweden inferred from
800 dendrochronological and historical archives, Climate Research, 29, 63-72, 2005.
801 Linderholm, H. W., Niklasson, M., and Molin, T.: Summer Moisture Variability in East Central
802 Sweden Since the Mid-Eighteenth Century Recorded in Tree Rings, Geografiska Annaler: Series A,
803 Physical Geography, 86, 277-287, 10.1111/j.0435-3676.2004.00231.x, 2004.
804 Linderholm, H. W., Björklund, J., Seftigen, K., Gunnarson, B. E., Grudd, H., Jeong, J.-H., Drobyshev,
805 I., and Liu, Y.: Dendroclimatology in Fennoscandia – from past accomplishments to future potential,
806 Climate of the Past, 6, 93-114, 2010.
807 Linderholm, H. W., Björklund, J., Seftigen, K., Gunnarson, B. E., and Fuentes, M.: Fennoscandia
808 revisited: a spatially improved tree-ring reconstruction of summer temperatures for the last 900 years,
809 Climate Dynamics, 45, 933-947, 10.1007/s00382-014-2328-9, 2014.
810 Madden, R. A., and Williams, J.: The Correlation between Temperature and Precipitation in the
811 United States and Europe, Monthly Weather Review, 106, 142-147, 10.1175/1520-
812 0493(1978)106<0142:tcbtap>2.0.co;2, 1978.
813 McCarroll, D., Loader, N. J., Jalkanen, R., Gagen, M. H., Grudd, H., Gunnarson, B. E., Kirchhefer, A.
814 J., Friedrich, M., Linderholm, H. W., Lindholm, M., Boettger, T., Los, S. O., Remmele, S., Kononov,
815 Y. M., Yamazaki, Y. H., Young, G. H., and Zorita, E.: A 1200-year multiproxy record of tree growth
816 and summer temperature at the northern pine forest limit of Europe, The Holocene, 23, 471-484,
817 10.1177/0959683612467483, 2013.
818 Melvin, T. M., and Briffa, K. R.: A "signal-free" approach to dendroclimatic standardisation,
819 Dendrochronologia, 26, 71-86, 10.1016/j.dendro.2007.12.001, 2008.
820 National Research Council: Surface Temperature Reconstructions for the Last 2,000 Years, The
821 National Academies Press, Washington, DC978-0-309-10225-4, 160, 2006.
822 Oglesby, R., Feng, S., Hu, Q., and Rowe, C.: The role of the Atlantic Multidecadal Oscillation on
823 medieval drought in North America: Synthesizing results from proxy data and climate models, Global
824 Planet Change, 84–85, 56-65, http://dx.doi.org/10.1016/j.gloplacha.2011.07.005, 2012.
825 Osborn, T. J.: Simulating the winter North Atlantic Oscillation: the roles of internal variability and
826 greenhouse gas forcing, Climate Dynamics, 22, 605-623, 10.1007/s00382-004-0405-1, 2004.
827 Otto-Bliesner, B. L., Brady, E. C., Fasullo, J., Jahn, A., Landrum, L., Stevenson, S., Rosenbloom, N.,
828 Mai, A., and Strand, G.: Climate Variability and Change since 850 CE: An Ensemble Approach with
829 the Community Earth System Model, Bulletin of the American Meteorological Society, 97, 735-754,
830 10.1175/bams-d-14-00233.1, 2016.
831 Sarojini, B. B., Stott, P. A., and Black, E.: Detection and attribution of human influence on regional
832 precipitation, Nature Clim. Change, 6, 669-675, 10.1038/nclimate2976, 2016.
833 Schmidt, G. A., Jungclaus, J. H., Ammann, C. M., Bard, E., Braconnot, P., Crowley, T. J., Delaygue,
834 G., Joos, F., Krivova, N. A., Muscheler, R., Otto-Bliesner, B. L., Pongratz, J., Shindell, D. T., Solanki,
835 S. K., Steinhilber, F., and Vieira, L. E. A.: Climate forcing reconstructions for use in PMIP

836 simulations of the last millennium (v1.0), Geosci. Model Dev., 4, 33-45, 10.5194/gmd-4-33-2011,
837 2011.
838 Seftigen, K., Linderholm, H. W., Drobyshev, I., and Niklasson, M.: Reconstructed drought variability
839 in southeastern Sweden since the 1650s, International Journal of Climatology, 33, 2449-2458,
840 10.1002/joc.3592, 2013.
841 Seftigen, K., Björklund, J., Cook, E. R., and Linderholm, H. W.: A tree-ring field reconstruction of
842 Fennoscandian summer hydroclimate variability for the last millennium, Climate Dynamics, 44, 3141-
843 3154, 10.1007/s00382-014-2191-8, 2014.
844 Seftigen, K., Cook, E., Linderholm, H., Fuentes, M., and Björklund, J.: The Potential of Deriving
845 Tree-Ring-Based Field Reconstructions of Droughts and Pluvials over Fennoscandia, Journal of
846 Climate, 28, 3453-3471, 10.1175/JCLI-D-1300734.s1, 2015.
847 Seneviratne, S. I., Corti, T., Davin, E. L., Hirschi, M., Jaeger, E. B., Lehner, I., Orlowsky, B., and
848 Teuling, A. J.: Investigating soil moisture–climate interactions in a changing climate: A review, Earth-
849 Science Reviews, 99, 125-161, http://dx.doi.org/10.1016/j.earscirev.2010.02.004, 2010.
850 Shindell, D. T., Schmidt, G. A., Mann, M. E., and Faluvegi, G.: Dynamic winter climate response to
851 large tropical volcanic eruptions since 1600, Journal of Geophysical Research: Atmospheres, 109, n/a-
852 n/a, 10.1029/2003JD004151, 2004.
853 Sigl, M., Winstrup, M., McConnell, J. R., Welten, K. C., Plunkett, G., Ludlow, F., Buntgen, U.,
854 Caffee, M., Chellman, N., Dahl-Jensen, D., Fischer, H., Kipfstuhl, S., Kostick, C., Maselli, O. J.,
855 Mekhaldi, F., Mulvaney, R., Muscheler, R., Pasteris, D. R., Pilcher, J. R., Salzer, M., Schupbach, S.,
856 Steffensen, J. P., Vinther, B. M., and Woodruff, T. E.: Timing and climate forcing of volcanic
857 eruptions for the past 2,500 years, Nature, 523, 543-549, 2015.
858 Taylor, K. E., Stouffer, R. J., and Meehl, G. A.: An Overview of CMIP5 and the Experiment Design,
859 Bulletin of the American Meteorological Society, 93, 485-498, 10.1175/bams-d-11-00094.1, 2012.
860 Thiéblemont, R., Matthes, K., Omrani, N.-E., Kodera, K., and Hansen, F.: Solar forcing synchronizes
861 decadal North Atlantic climate variability, Nature communications, 6, 8268, 2015.
862 Thomson, D. J.: Spectrum estimation and harmonic analysis, Proceedings of the IEEE, 70, 1055-1096,
863 10.1109/PROC.1982.12433, 1982.
864 Thornthwaite, C. W.: An Approach Toward a Rational Classification of Climate, Soil Science, 66, 77,
865 1948.
866 Tolwinski-Ward, S., Evans, M. N., Hughes, M. K., and Anchukaitis, K. J.: An efficient forward model
867 of the climate controls on interannual variation in tree-ring width, Climate Dynamics, 36, 2419-2439,
868 10.1007/s00382-010-0945-5, 2011.
869 Trenberth, K. E.: Changes in precipitation with climate change, Climate Research, 47, 123-138,
870 10.3354/cr00953, 2011.
871 van Oldenborgh, G. J., and Van Ulden, A. A. D.: On the relationship between global warming, local
872 warming in the Netherlands and changes in circulation in the 20th century, International Journal of
873 Climatology, 23, 1711-1724, 10.1002/joc.966, 2003.
874 Vicente-Serrano, S. M., Beguería, S., and López-Moreno, J. I.: A Multiscalar Drought Index Sensitive
875 to Global Warming: The Standardized Precipitation Evapotranspiration Index, Journal of Climate, 23,
876 1696-1718, 10.1175/2009jcli2909.1, 2010.
877 Vicente-Serrano, S. M., Gouveia, C., Camarero, J. J., Beguería, S., Trigo, R., López-Moreno, J. I.,
878 Azorín-Molina, C., Pasho, E., Lorenzo-Lacruz, J., Revuelto, J., Morán-Tejeda, E., and Sanchez-
879 Lorenzo, A.: Response of vegetation to drought time-scales across global land biomes, Proceedings of
880 the National Academy of Sciences, 110, 52-57, 10.1073/pnas.1207068110, 2013.
881 Watanabe, S., Hajima, T., Sudo, K., Nagashima, T., Takemura, T., Okajima, H., Nozawa, T., Kawase,
882 H., Abe, M., Yokohata, T., Ise, T., Sato, H., Kato, E., Takata, K., Emori, S., and Kawamiya, M.:
883 MIROC-ESM 2010: model description and basic results of CMIP5-20c3m experiments, Geosci.
884 Model Dev., 4, 845-872, 10.5194/gmd-4-845-2011, 2011.
885 Wigley, T. M. L., Briffa, K. R., and Jones, P. D.: On the Average Value of Correlated Time Series,
886 with Applications in Dendroclimatology and Hydrometeorology, Journal of Climate and Applied
887 Meteorology, 23, 201-213, 10.1175/1520-0450(1984)023<0201:otavoc>2.0.co;2, 1984.
888 Wilson, R., Miles, D., Loader, N. J., Melvin, T., Cunningham, L., Cooper, R., and Briffa, K.: A
889 millennial long March–July precipitation reconstruction for southern-central England, Climate
890 Dynamics, 10.1007/s00382-012-1318-z, 2012.

Wilson, R., Anchukaitis, K., Briffa, K. R., Büntgen, U., Cook, E., D'Arrigo, R., Davi, N., Esper, J., Frank, D., Gunnarson, B., Hegerl, G., Helama, S., Klesse, S., Krusic, P. J., Linderholm, H. W., Myglan, V., Osborn, T. J., Rydval, M., Schneider, L., Schurer, A., Wiles, G., Zhang, P., and Zorita, E.: Last millennium northern hemisphere summer temperatures from tree rings: Part I: The long term context, Quaternary Science Reviews, 134, 1-18, 10.1016/j.quascirev.2015.12.005, 2016.

Wu, P., Christidis, N., and Stott, P.: Anthropogenic impact on Earth/'s hydrological cycle, Nature Clim. Change, 3, 807-810, 2013.

Wu, T., Song, L., Li, W., Wang, Z., Zhang, H., Xin, X., Zhang, Y., Zhang, L., Li, J., Wu, F., Liu, Y., Zhang, F., Shi, X., Chu, M., Zhang, J., Fang, Y., Wang, F., Lu, Y., Liu, X., Wei, M., Liu, Q., Zhou, W., Dong, M., Zhao, Q., Ji, J., Li, L., and Zhou, M.: An overview of BCC climate system model development and application for climate change studies, Journal of Meteorological Research, 28, 34-56, 10.1007/s13351-014-3041-7, 2014.

Zhang, H., Yuan, N., Esper, J., Werner, J. P., Xoplaki, E., Büntgen, U., Treydte, K., and Luterbacher, J.: Modified climate with long term memory in tree ring proxies, Environmental Research Letters, 10, 084020, 10.1088/1748-9326/10/8/084020, 2015.

Zhang, X., Zwiers, F. W., Hegerl, G. C., Lambert, F. H., Gillett, N. P., Solomon, S., Stott, P. A., and Nozawa, T.: Detection of human influence on twentieth-century precipitation trends, Nature, 448, 461-465, 2007.

Tables and figures

Table I. CMIP5/PMIP3 model description.

Model Name	**Resolution [Atmosphere]**	**Resolution [Ocean]**	**Reference**
CCSM4	192 x 288	384 x 320	Landrum et al. (2012)
CESM1	96 x 144	384 x 320	Lehner et al. (2015)
IPSL-CM5A-LR	96 x 96	149 x 182	Dufresne et al. (2013)
MIROC-ESM	64 x 128	192 x 256	Watanabe et al. (2011)
MPI-ESM-P	96 x 192	220 x 256	Jungclaus et al. (2014)
BCC-CSM1-1	64 x 128	232 x 360	Wu et al. (2014)

926 **Table II:** Tree-ring network description.

Site	Coord.	Time coverage	Standardization method	MSL[3]	Source
Eastern Finland	61.87N, 28.90E	535 -2002 CE	RCS[1]	147 yrs	Helama et al. (2009) Online resource: http://lustiag.pp.fi/Saima/dendrotieto.htm Date access: January 2013
Gotland Sweden	57.49N, 18.41E	1127-2011 CE	RCS	130 yrs	Investigator: Schweingruber, F.H. Online resource: https://www.ncdc.noaa.gov/paleo/study/4427 Date access: January 2013 Updated in Seftigen et al. (2015)
Jondalen Norway	59.71N, 9.53E	1185 -2011 CE	RCS	165 yrs	Investigator: Briffa, K. Online resource: https://www.ncdc.noaa.gov/paleo/study/2826 Date access: January 2013 Updated in Seftigen et al. (2015)
Baljåsen Sweden	59.04N, 12.27E	1686-2002 CE	SF2[2]	174 yrs	Seftigen et al. (2015)
Björbo Sweden	60.27N, 14.44E	1450-2011 CE	SF	177 yrs	Investigator: Axelson, T. Online resource: https://www.ncdc.noaa.gov/paleo/study/2667 Date access: January 2013
Ekhultebergen Sweden	57.45N, 13.50E	1705-2008 CE	SF1	215 yrs	Seftigen et al. (2015)
Fårhagsberget Sweden	58.08N, 16.14E	1621-2011 CE	SF1	262 yrs	Seftigen et al. (2015)
Helvetets håla Sweden	57.14N, 16.14E	1691-2011 CE	SF1	255 yrs	Seftigen et al. (2015)
Halle-Vagnaren Sweden	57.17N, 15.17E	1718-2009 CE	SF3	186 yrs	Seftigen et al. (2015)
Hornslandet Sweden	59.01N, 11.08E	1590-2011 CE	SF1	270 yrs	Seftigen et al. (2015)
Korphålorna Sweden	61.43N, 17.00E	1790-2011 CE	SF1	199 yrs	Seftigen et al. (2015)
Myrkaby Sweden	57.45N, 15.23E	1669-2011 CE	SF2	294 yrs	Seftigen et al. (2015)
Nämndö Sweden	59.52N, 16.56E	1582-1995 CE	SF1	123 yrs	Investigator: Larsson, L. Online resource: https://www.ncdc.noaa.gov/paleo/study/3869 Date access: January 2013
Valekleven-Ombo Sweden	59.11N, 18.41E	1578-2011 CE	SF1	225 yrs	Seftigen et al. (2015)
Putbergen Sweden	58.37N, 14.32E	1734-2008 CE	SF1	188 yrs	Seftigen et al. (2015)
Salboknös Sweden	59.11N, 16.55E	1486-2011 CE	SF2	357 yrs	Seftigen et al. (2015)
Särö Sweden	61.92N, 11.93E	1712-2002 CE	SF3	176 yrs	Seftigen et al. (2015)
Sisshammer Sweden	59.46N, 14.54E	1661-2003 CE	SF	74 yrs	Investigator: Andreason, T. Online resource: https://www.ncdc.noaa.gov/paleo/study/2663 Date access: January 2013
Skärmarbodabergen Sweden	57.51N, 11.93E	1600-2002 CE	SF3	160 yrs	Seftigen et al. (2015)
Skitåsen Sweden	59.09N, 18.02E	1672-2011 CE	SF2	285 yrs	Seftigen et al. (2015)
Skuleskogen Sweden	59.26N, 15.07E	1448-2011 CE	SF	181 yrs	Seftigen et al. (2015)
Sörknatten Sweden	59.22N, 15.29E	1762-2009 CE	SF3	197 yrs	Seftigen et al. (2015)
Tjurhults mosse Sweden	63.06N, 18.29E	1655-2011 CE	SF2	268 yrs	Seftigen et al. (2015)
Tjusthult Sweden	58.55N, 12.27E	1681-2011 CE	SF1	221 yrs	Seftigen et al. (2015)
Tyresta Sweden	59.52N, 14.71E	1609-2010 CE	SF1	198 yrs	Linderholm and Molin (2005) Updated in Seftigen et al. (2015)

927 [1] RCS: Regional Curve Standardization;

928 [2] SF: Signal-Free Standardization. The number after the abbreviation indicates the PCA cluster number (Fig. S2);

929 [3]MSL: Mean Segment Length.

930 **Table III.** Event years used in the Superposed Epoch Analysis (Fig. 4). The event lists are composed
931 of the 20 strongest eruptions from each record.

Source	**Event years (CE)**
Gao et al. (2008) (sulfate aerosol > 15 Tg)	1167, 1176, 1195, 1227, 1258, 1284, 1328, 1452, 1459, 1584, 1600, 1641, 1719, 1783, 1809, 1815, 1831, 1835, 1991
Crowley and Unterman (2013) (AOD > 0.13)	1229, 1258, 1259, 1286, 1287, 1456, 1457, 1600, 1601, 1641, 1695, 1696, 1809, 1810, 1815, 1816, 1817, 1884, 1992
Sigl et al. (2015) (global forcing < 5.86 W/m^2)	1108, 1171, 1191, 1230, 1258, 1276, 1286, 1345, 1453, 1458, 1601, 1641, 1695, 1783, 1809, 1815, 1832, 1836, 1992

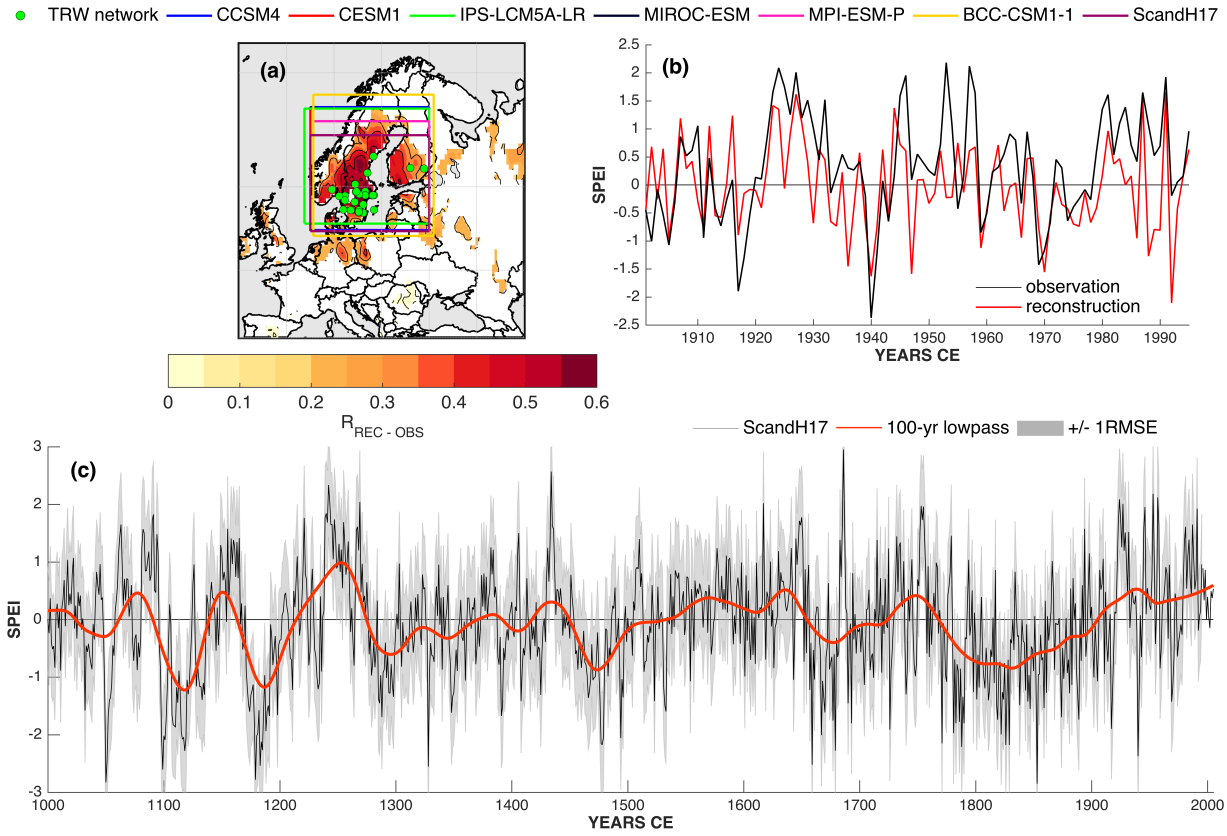

Figure 1: Average regional warm-season SPEI time series reconstructed from tree-rings. (a) Location of the tree-ring network used for regional reconstruction and the extent of the CMIP5/PMIP3 model precipitation and temperature grids used to derive regional SPEI estimates. Shaded contours display the correlation ($p < 0.1$) between the tree-ring reconstruction and fields of instrumental SPEI data over the 1901-1995 period; (b) average regional reconstructed and instrumental 20th century 2-month June SPEI; (c) average regional SPEI nested reconstruction, with the +/- 1RMSE of the regression equations outlined in grey shading. A smoothed version of the reconstruction using a 100-year loess smooth is shown in red. Reconstruction assessment metrics are provided in supplementary materials (Fig. S4).

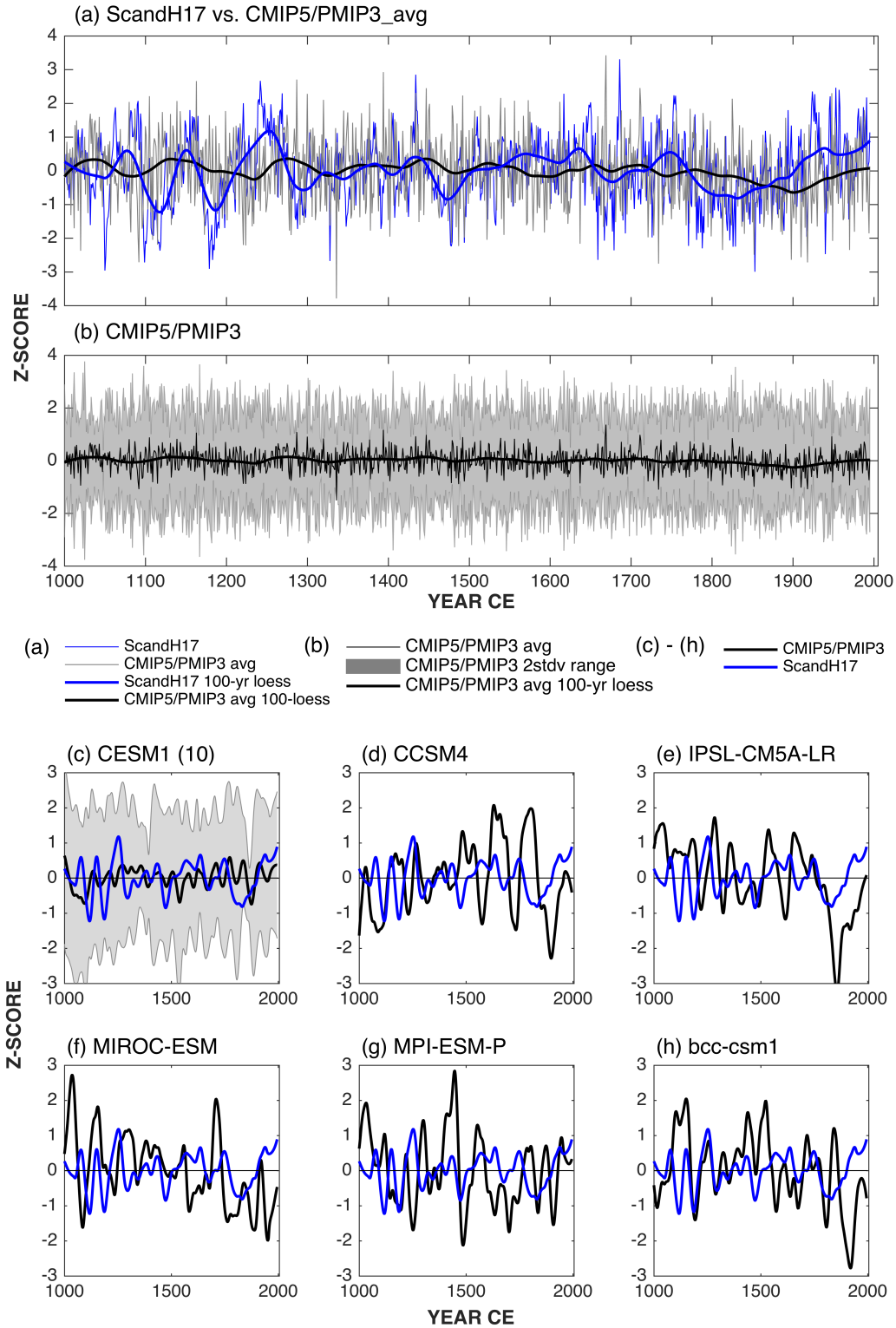

Figure 2: Comparison of reconstructed SPEI with forced model runs. (a) The reconstruction versus the mean of the six CMIP5/PMIP3 models transformed into standard normal deviates (z-scores) over the 1000-1995 CE period and smoothed with 100-year loess filter; (b) multimodel mean and the two standard deviation range (shading) of the six GCMs; (c) mean and two standard deviation (shading) of CESM1 ten smoothed and z-scored ensemble members (blue) together; (d) – (h) the

reconstruction (blue) versus individual model runs (black). All time series have been smoothed with 100-year loess filter and then z-scored over the 1000-1995 CE period.

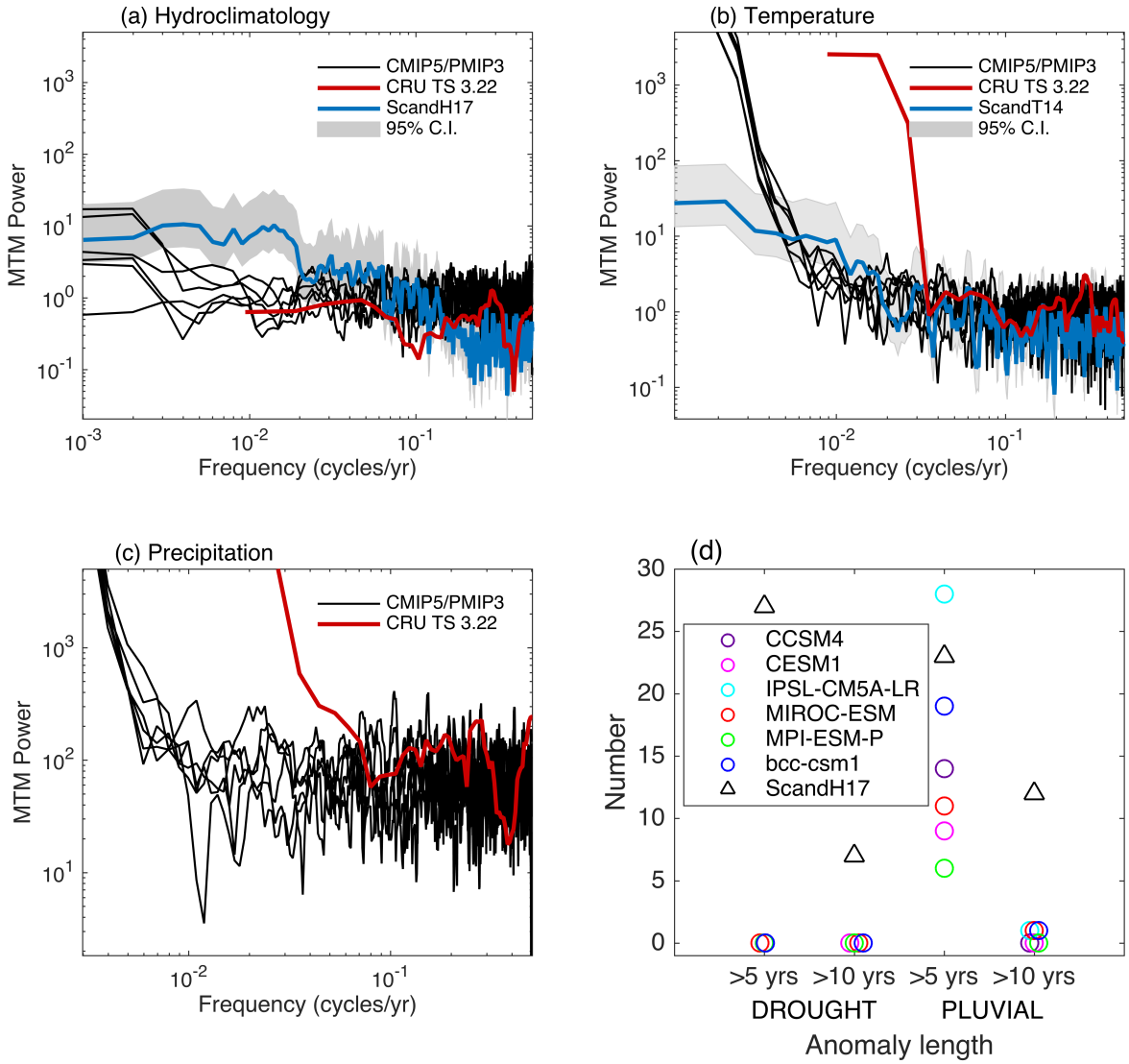

Figure 3: Spectral properties (multi-taper approach, 4 tapers) of (a) SPEI, (b) temperature and (c) precipitation over the common 1100-1995 period. For SPEI and temperature, the spectral properties of individual GCMs (r1i1p1 ensemble) are compared to those of the tree-ring ScandH17 and ScandT14 reconstructions and regionally averaged instrumental CRU TS 3.22 data. Shaded areas show the 95% confidence interval of the reconstruction spectra. (d) The number of droughts and pluvials in the reconstructed and simulated time series that are > 5 and >10 years in duration. Spectral properties of the individual models are provided in Fig. S7.

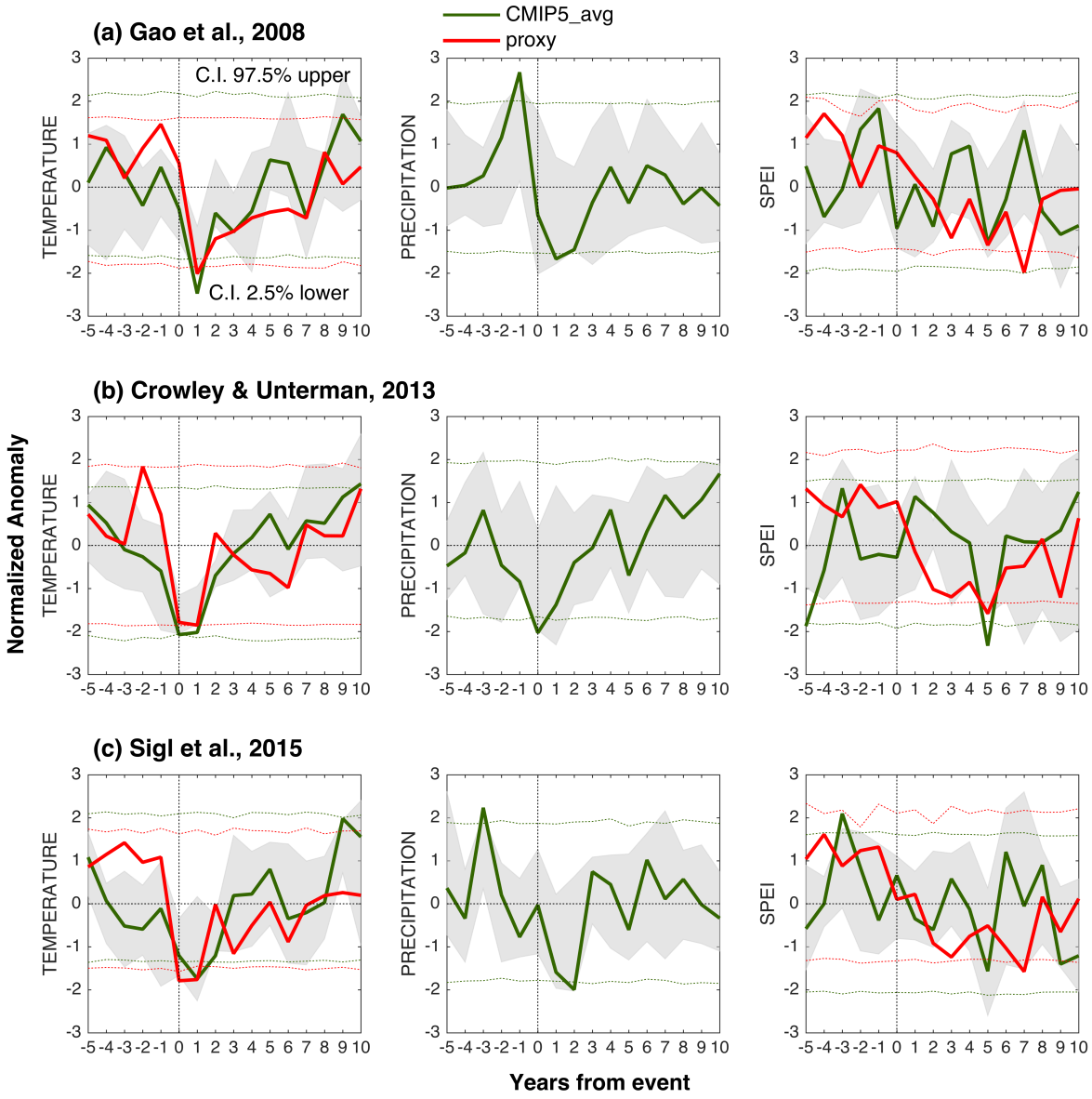

Figure 4: Modeled and reconstructed hydroclimate response to eruptions. Superposed epoch analysis using the 20 largest eruption years from the (a) Gao et al. (2008), (b) Crowley and Unterman (2013), and (c) Sigl et al. (2015). Table III lists the event years used in the analysis. Grey shading indicate the range of modeled hydroclimate response from the six GCMs. Confidence intervals (C.I.) are derived from bootstrap resampling (N = 10 000).

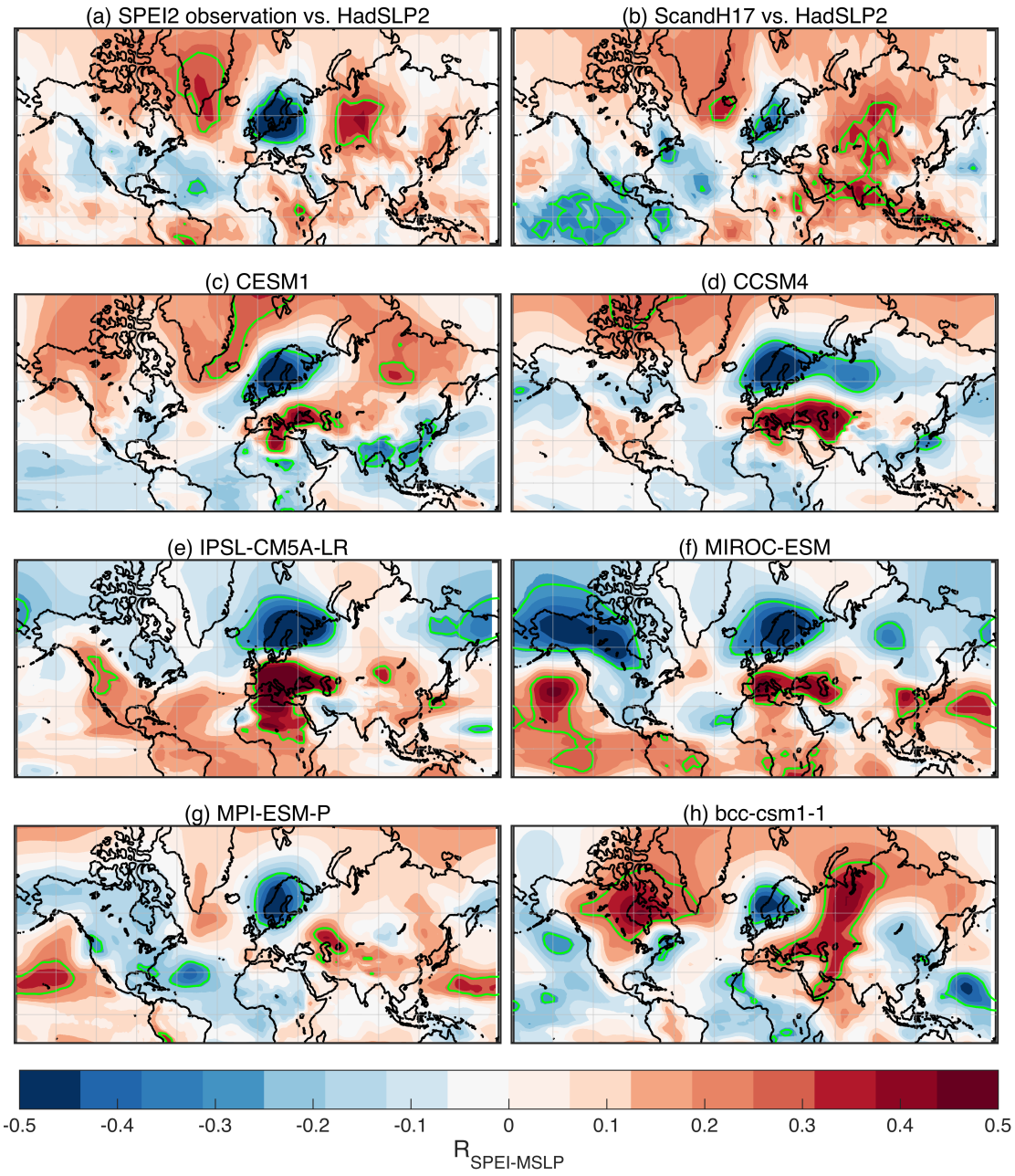

Figure 5: Spatial distribution of correlation coefficient of northern European warm season hydroclimate and mean sea level pressure (MSLP). Association between regional drought index and sea level pressure over the 1950-1995 period. (a) observational, (b) ScandH17, (c)-(g) model based results (including r1i1p1 ensemble only). Regions with significant ($p < 0.05$) correlations are outlined in green contours.

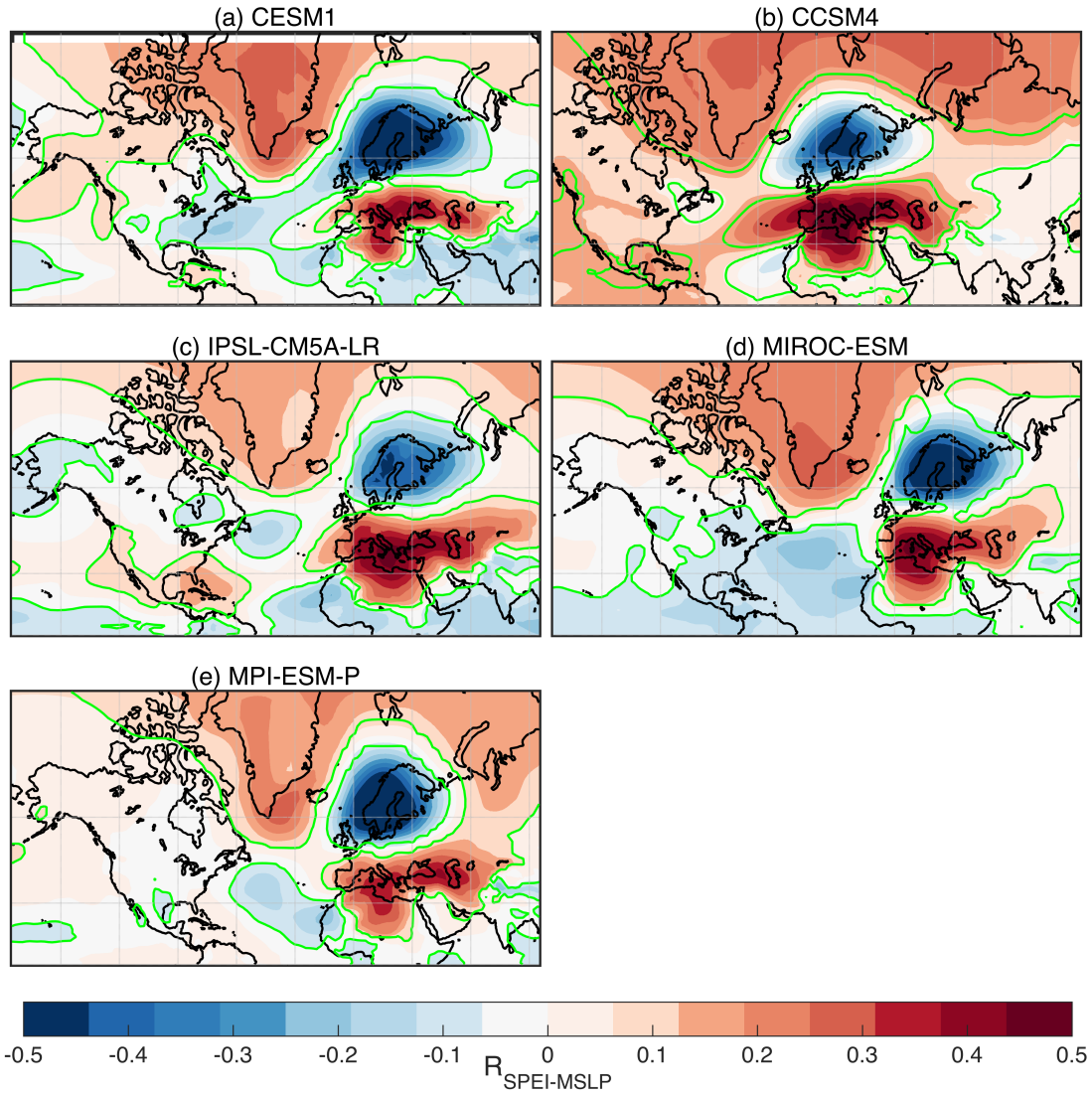

Figure 6: Spatial distribution of correlation coefficient of northern European warm season hydroclimate and mean sea level pressure (MSLP). Same as Fig. 5, but for the 850-1849 CE period.

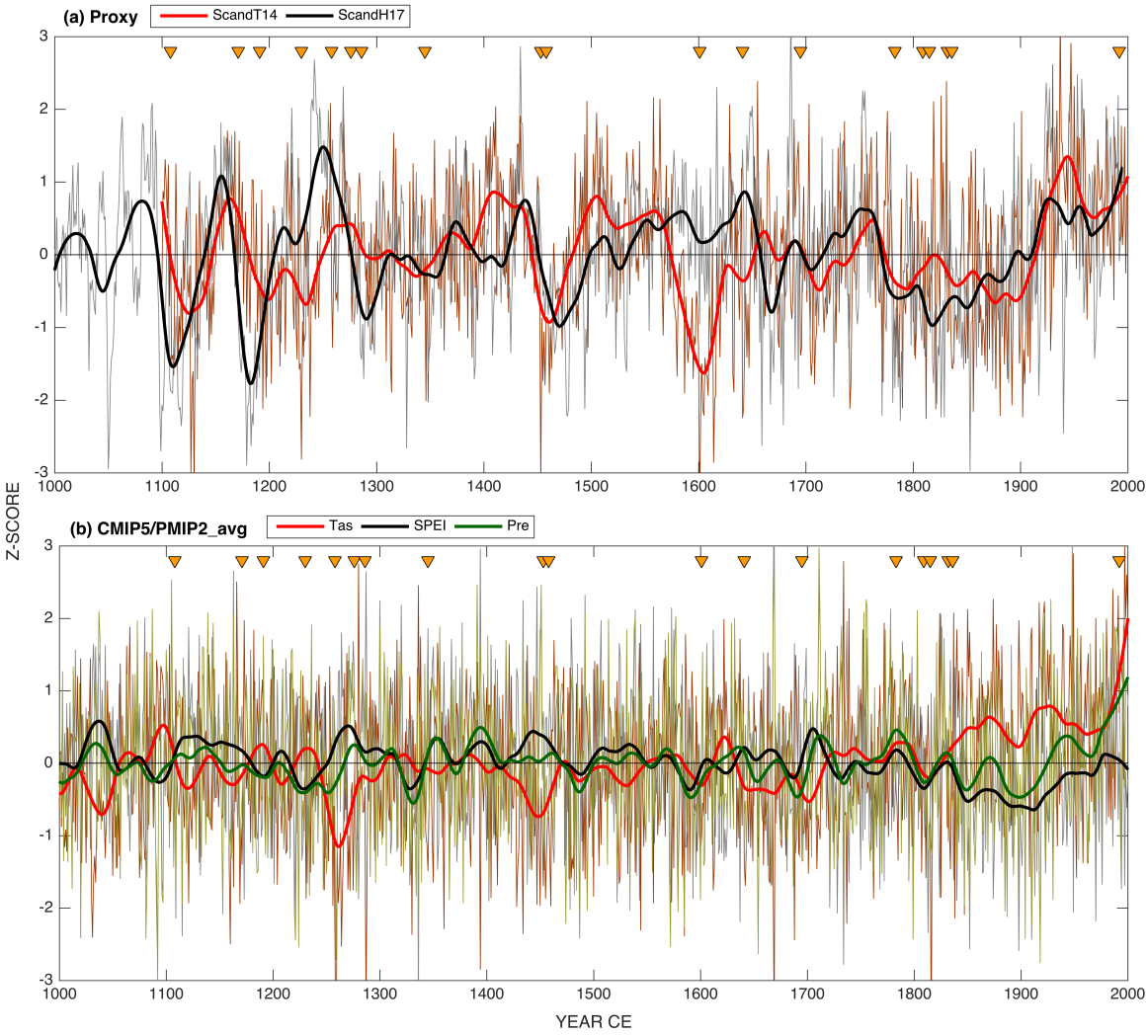

Figure 7: Time series of (a) ScandH17 and ScandT14, and (b) GCM (r1i1p1 ensemble) average temperature, precipitation and SPEI. Smoothed time-series using a 50-year loess filter are shown as thick lines. Individual model data are provided in supplementary material (Fig. S8). The years with volcanic eruptions from Table III are indicated by triangle glyphs.

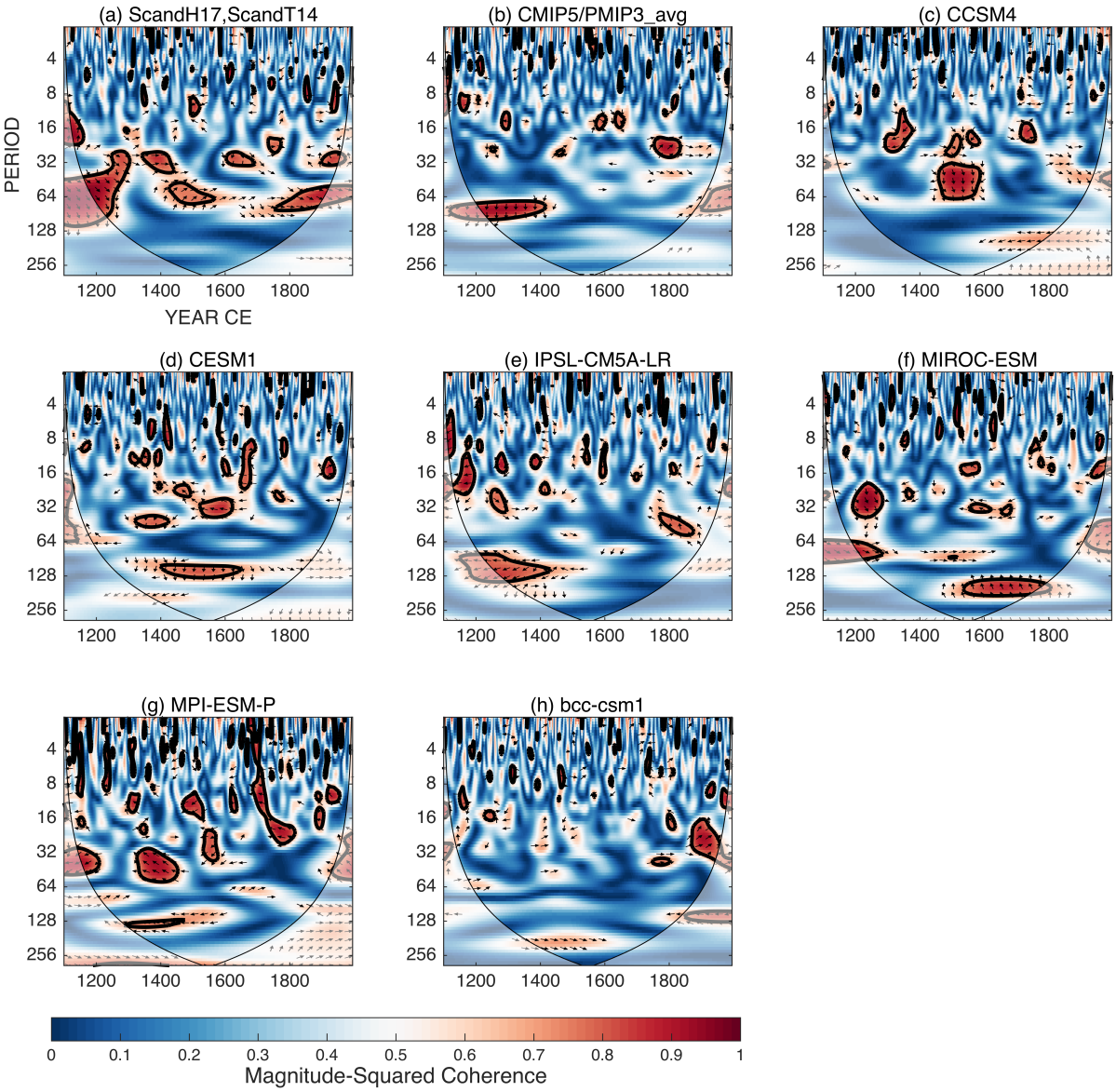

Figure 8: Squared wavelet coherence and phase between (a) ScandH17 and ScandT14, and (b) – (h) CMIP5/PMIP3 simulations of temperature and rainfall. The arrows indicate the relative phase relationship between two series; right (left) pointing arrow indicates in-phase (180 degrees out of phase) relationship. Significant coherence at 95% significance level is shown as thick contour.